Nuclear deformation across nuclear chart in the covariant density functional framework

Anatoli Afanasjev
Mississippi State University (MSU), USA

1. **Motivation and theoretical framework**
2. **What defines the deformation: the connection to underlying single-particle structure.**
3. **A global view with assessment of theoretical uncertainties.**
4. **Differential charge radii: when they reveal a deformation**
5. **Rotation in nuclei: a clear signal of deformation**
6. **Survey of octupole deformation**
7. **The challenge of superheavy nuclei**
8. **The consequences for ^{96}Zr**
9. **Conclusions**

Motivation and theoretical framework

Approximations in the modelling of nuclear many-body problem.

General approach (DFT level)

Non-relativistic Schrodinger equation: Skyrme and Gogny DFT

Relativistic Dirac equation: covariant DFT (CDFT)

Range of interaction

Zero range - point coupling models in CDFT (no mesons)
- Skyrme DFT

Finite range - meson exchange models in CDFT
- Gogny DFT

Effective density dependence

CDFT :
- explicit (DD-ME2, DD-PC1)
- non-linear (through the powers of mesons) (NL1, NL3*)

Skyrme and Gogny DFTs: different prescriptions for density dependence

Covariant density functional theory (CDFT)

The nucleons interact via the exchange of effective mesons →
→ **effective Lagrangian**

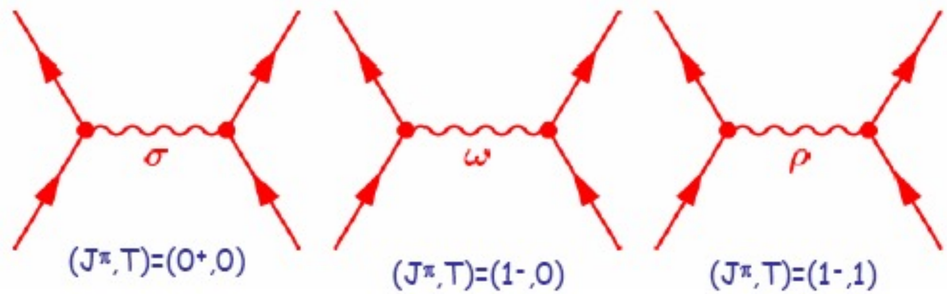

Long-range attractive scalar field

Short-range repulsive vector field

Isovector field

$$E_{\mathrm{RMF}}[\hat{\rho}, \phi_m] = \mathrm{Tr}[(\boldsymbol{\alpha p} + \beta m)\hat{\rho}] \pm \int \left[\frac{1}{2}(\nabla \phi_m)^2 + U(\phi_m)\right] \mathrm{d}^3 r + \mathrm{Tr}[(\Gamma_m \phi_m)\hat{\rho}]$$

density matrix $\hat{\rho}$ $\qquad$ $\phi_m \equiv \{\sigma, \omega^\mu, \vec{\rho}^\mu, A^\mu\}$ - meson fields

$$\boxed{\hat{h} = \frac{\delta E}{\delta \hat{\rho}}}$$ **Mean field**

$$\boxed{\hat{h}|\varphi_i\rangle = \varepsilon_i |\varphi_i\rangle}$$ **Eigenfunctions**

Dirac equation for fermions

$$\{\vec{\alpha}\vec{p} + V + \beta(m+S)\}\,\Psi_i = \epsilon_i \Psi_i$$

$$\Psi_i = \begin{pmatrix} f_i(r) \\ i g_i(r) \end{pmatrix} = \begin{pmatrix} \text{large components} \\ \text{small components} \end{pmatrix}$$

Klein-Gordon equations for mesons

$$\{-\Delta + m_\sigma^2\}\,\sigma = -g_\sigma \rho_s - g_2 \sigma^2 - g_3 \sigma^3$$

$$\{-\Delta + m_\omega^2\}\,\omega_0 = g_\omega \rho_v$$

V ~ 350 MeV/nucleon
S ~ - 400 MeV/nucleon
U ~ - 50 MeV/nucleon

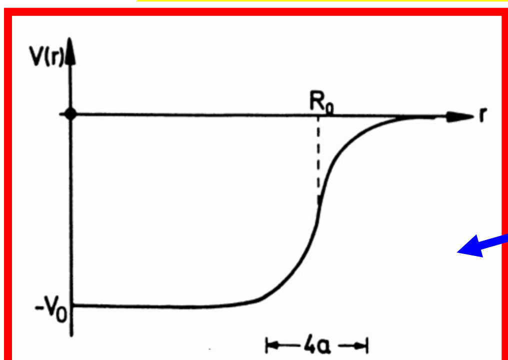

U=S+V

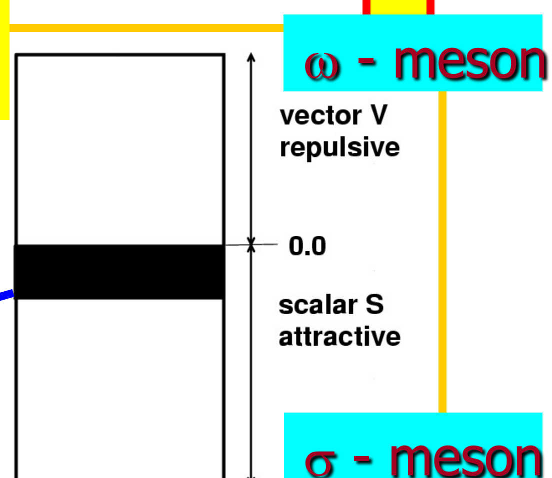

Densities

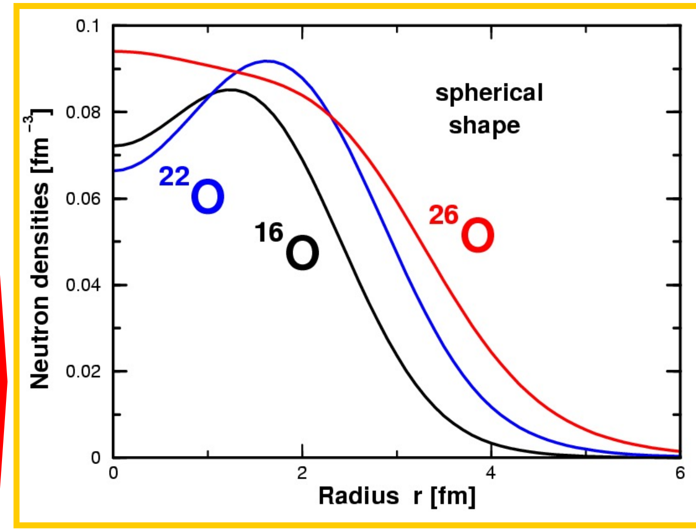

Single-particle energies

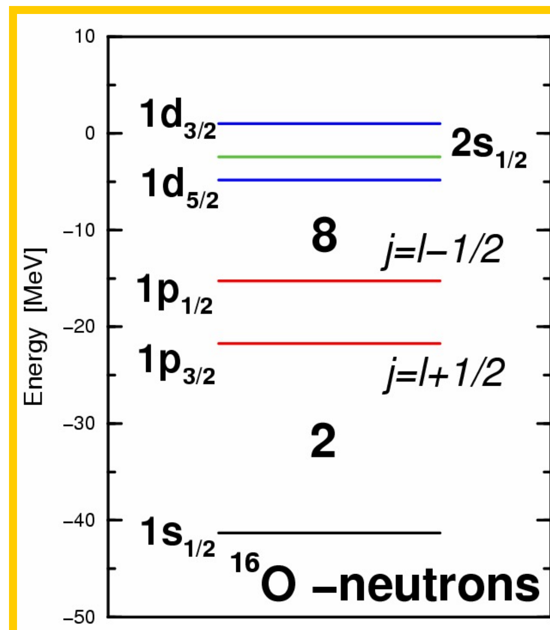

Why relativistic treatment based on Dirac equation?

No relativistic kinematics,

HOWEVER

1. **Spin** degrees of freedom as well as **spin-orbit interaction** are obtained in a natural way (no extra parameters).

Spin-orbit splittings are properly described

E.Litvinova and AA. PRC 84, 014305 (2011).

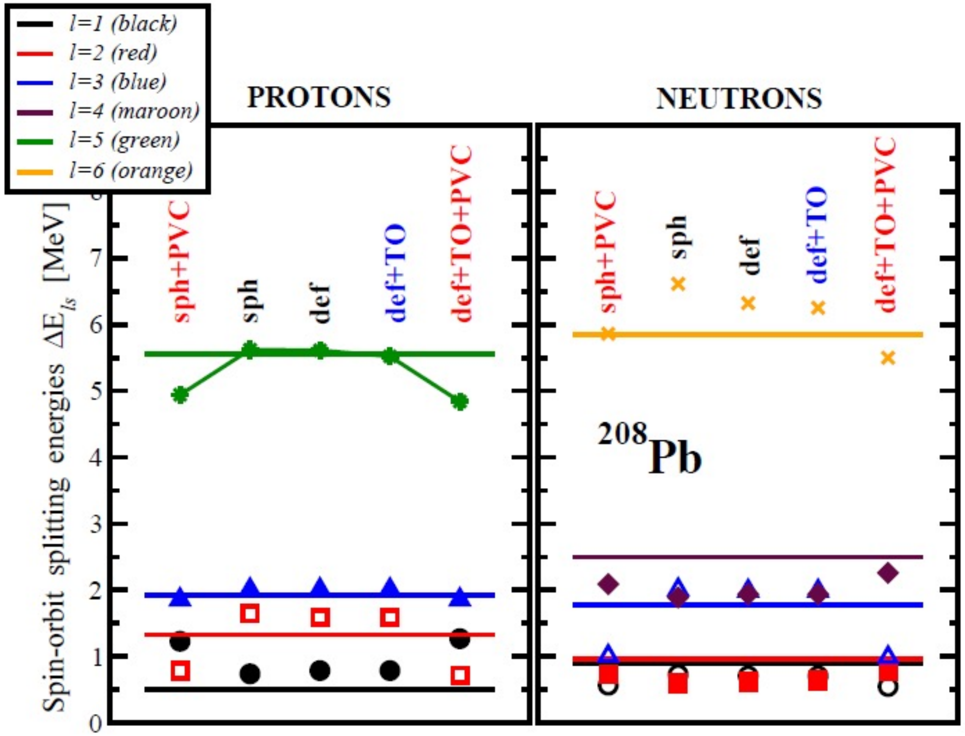

2. Time-odd mean fields are defined via Lorentz covariance → very weak dependence on the RMF parametrization.

AA, H. Abusara, PRC 81, 014309 (2010).

Important for odd-mass and rotating nuclei.

Basic structure of CEDFs and their density dependence

The basic idea comes from ab initio calculations.
Density dependent coupling constants include
Brueckner correlations and three-body forces

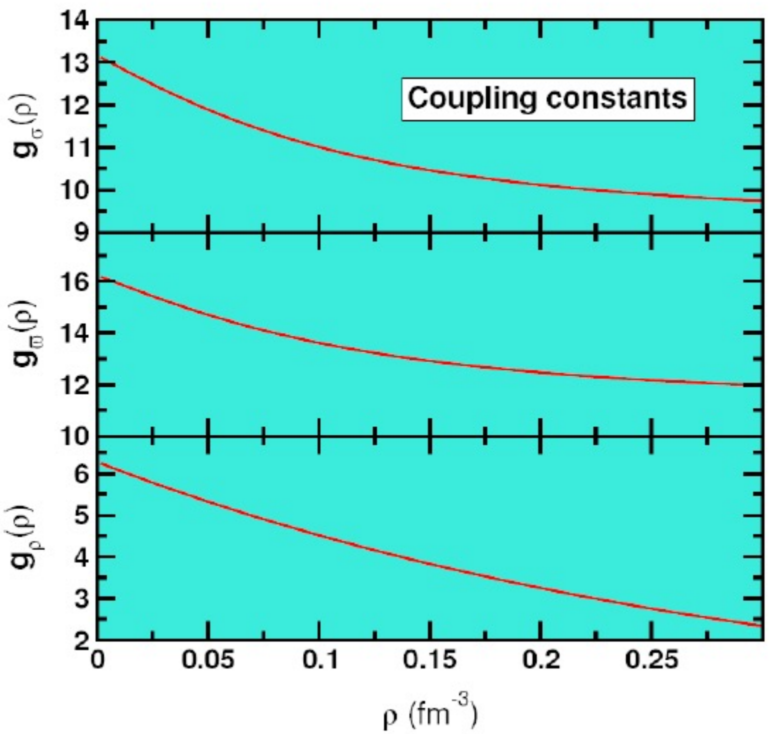

Effective interactions with medium-dependent couplings:

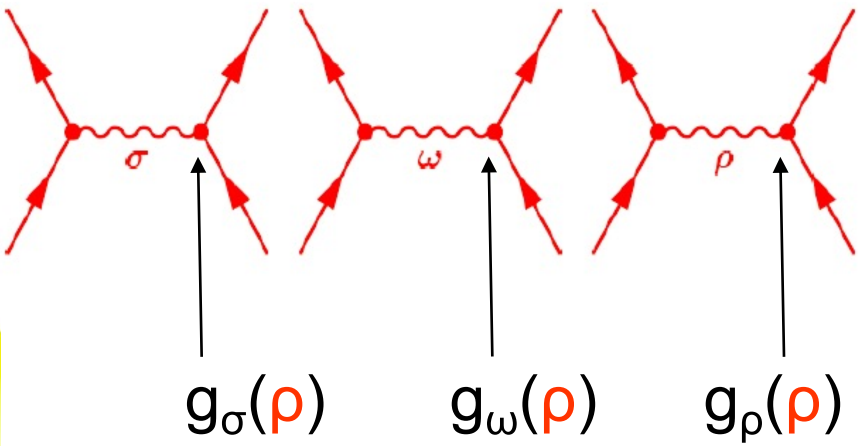

Remove mesons → point coupling models with derivative terms

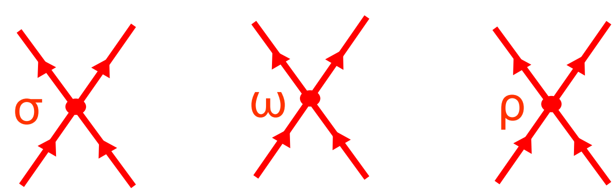

Relativistic Hartree-Bogoliubov (RHB) framework

$$\begin{pmatrix} h_D - \lambda & \Delta \\ -\Delta^* & -h_D^* + \lambda \end{pmatrix} \begin{pmatrix} U \\ V \end{pmatrix}_k = E_k \begin{pmatrix} U \\ V \end{pmatrix}_k$$

The separable version of the finite range Brink-Booker part of the Gogny D1S force is used in the particle-particle channel

$$V(\boldsymbol{r}_1, \boldsymbol{r}_2, \boldsymbol{r}_1', \boldsymbol{r}_2') = \\ = -f\, G\delta(\boldsymbol{R} - \boldsymbol{R}')P(r)P(r')\frac{1}{2}(1 - P^\sigma)$$

The global results for even-even nuclei are available in tabulated form at:

S. Agbemava, AA, D, Ray, P.Ring, PRC **89**, 054320 (2014)
includes complete DD-PC1 mass table as supplement

Mass Explorer at FRIB (the results for DD-PC1, NL3*, DD-ME2, and DD-MEδ)

http://massexplorer.frib.msu.edu/content/DFTMassTables.html

The NL3*, PC-PK1, DD-ME2, DD-PC1 and DD-MEδ covariant energy density functionals are used in order to assess the dependence of results on the functional and underlying single-particle structure and assess systematic theoretical uncertainties

What defines the deformation: the connection to underlying single-particle structure

Deformation parameters and nuclear shapes

Quadrupole deformation parameter:

$$\beta_2 = Q_{20} \Big/ \left(\sqrt{\frac{16\pi}{5}} \frac{3}{4\pi} A R_0^2 \right)$$

Octupole deformation parameter:

$$\beta_3 = Q_{30} \Big/ \left(\sqrt{\frac{16\pi}{7}} \frac{3}{4\pi} A R_0^3 \right)$$

where $R_0 = 1.2 A^{1/3}$

Hexadecapole deformation parameter:

$$Q_{40} = 8 \sqrt{\frac{4\pi}{9}} \frac{3}{4\pi} Z R_0^4 \beta_4$$

Multipole moments

$$Q_{20} = \langle 2z^2 - x^2 - y^2 \rangle,$$

$$Q_{30} = \langle z(2z^2 - 3x^2 - 3y^2) \rangle$$

Axial symmetric shapes: $\beta_3 = 0$

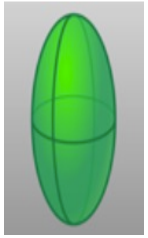
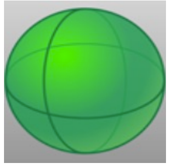
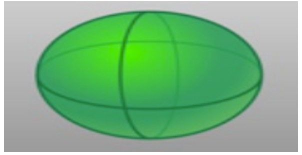

Oblate $\beta_2 < 0$	Spherical $\beta_2 = 0$	Prolate $\beta_2 > 0$

Axial asymmetric (octupole) shapes: $\beta_2 \neq 0,\ \beta_3 \neq 0$

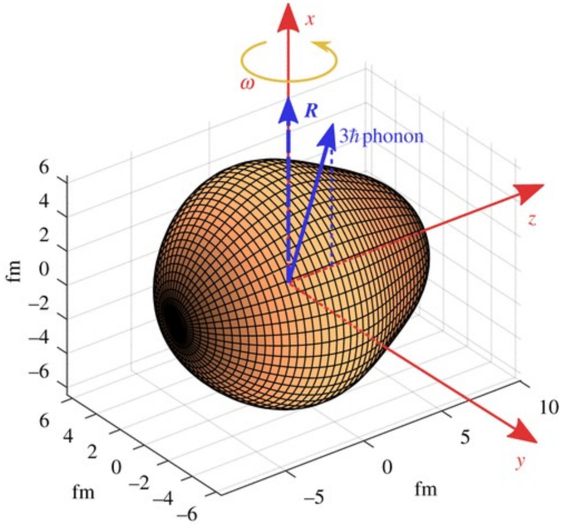

Figure from P.A.Butler, Proc.R.Soc. A476,20200202

$$E_{tot} = E_{LD} + \delta E_{shell} + E_{pair}$$

liquid drop

quantum (shell) correction

pairing

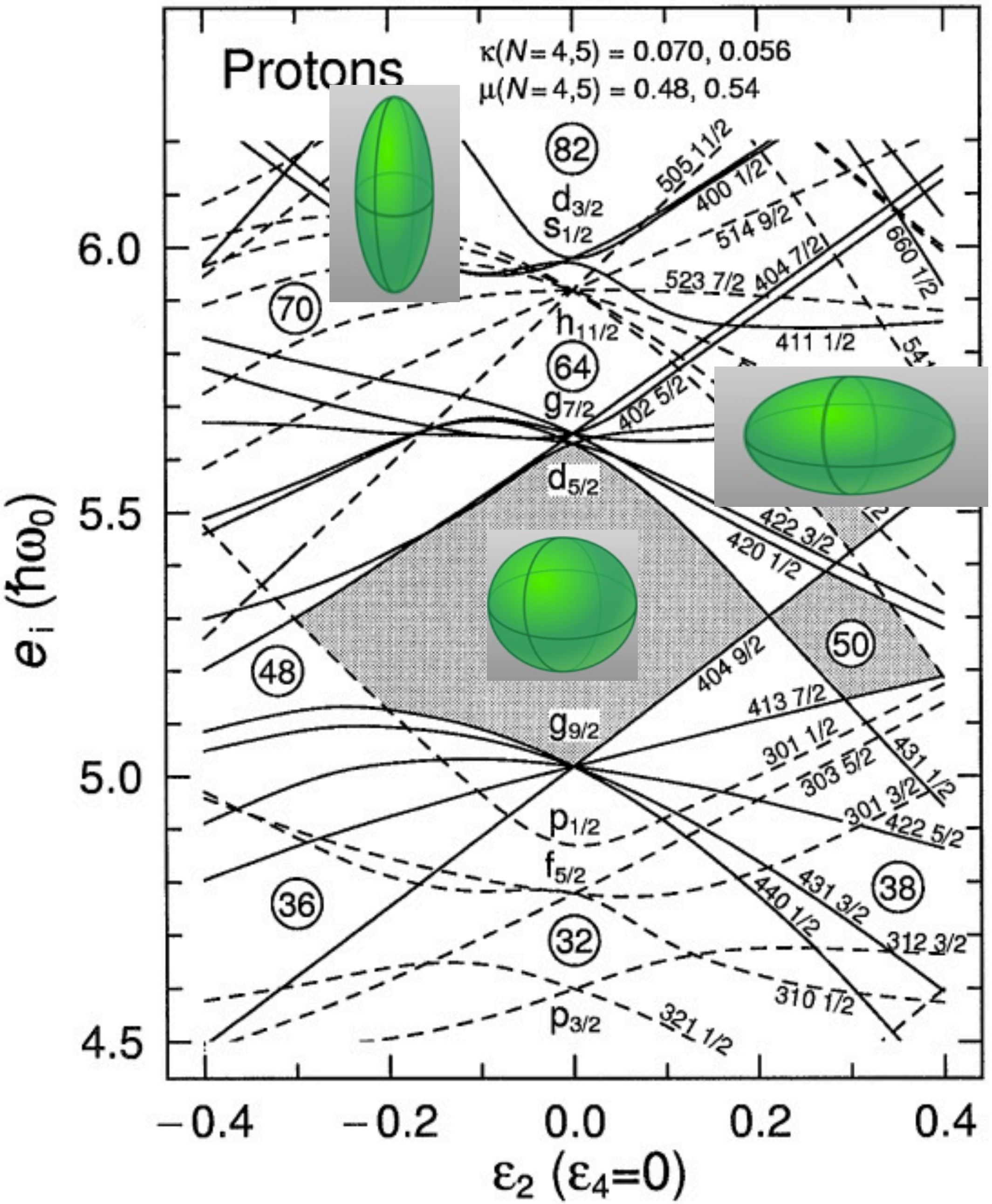

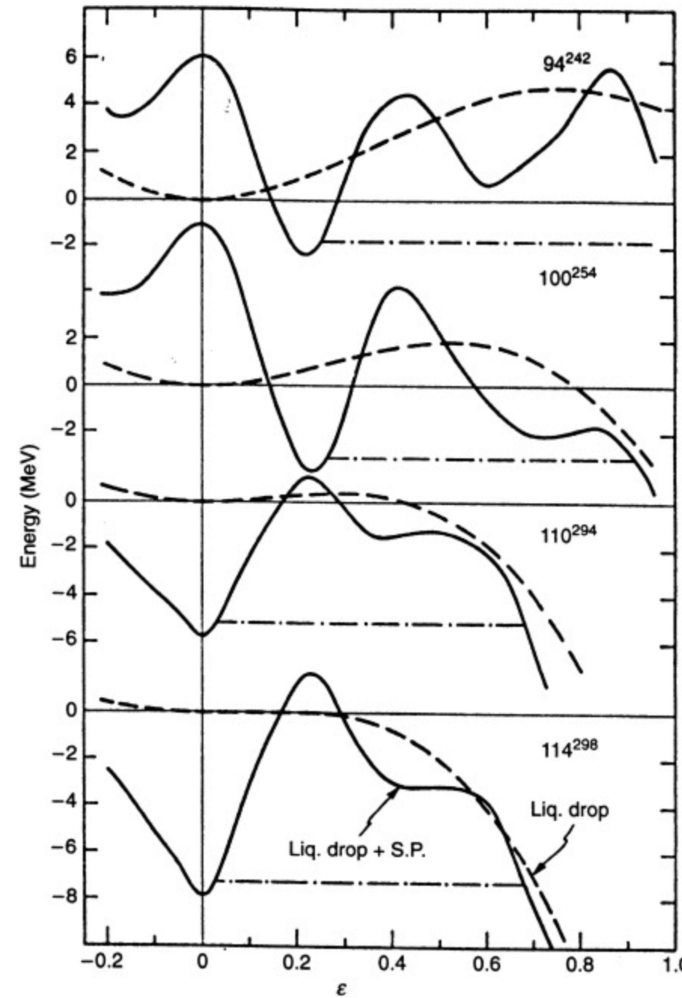

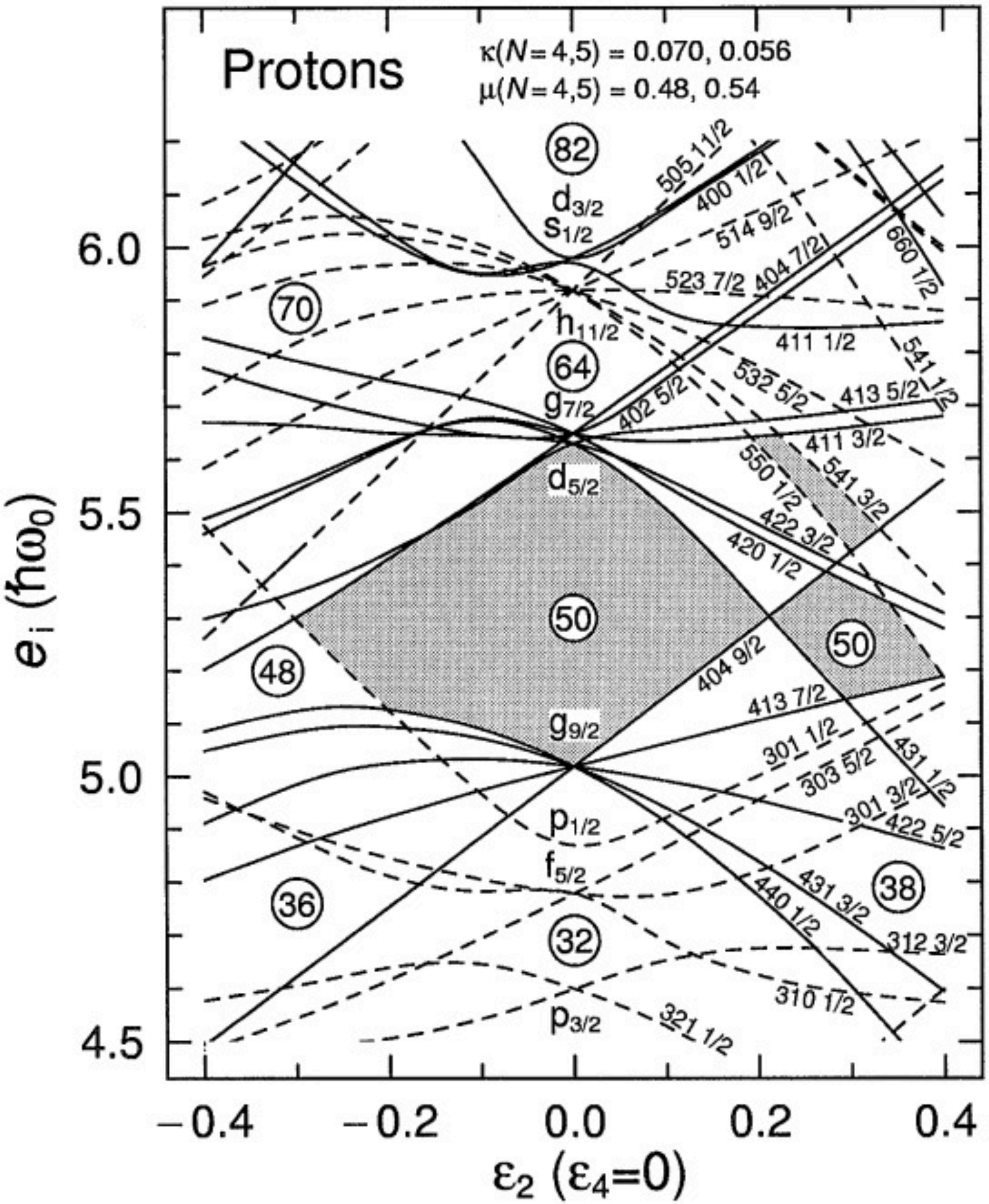

$$H = \sum_{i=1}^{A} h(\vec{r}_i) + \cancel{\sum_{i \neq j = 1}^{A} V(\vec{r}_i, \vec{r}_j)}$$

Independent particle motion model

$$h(\vec{r}) = -\frac{\hbar^2}{2m}\nabla_i^2 + V(\vec{r})$$

Hamiltonian for modified harmonic oscillator potential

$$h(\vec{r}) = -\frac{\hbar^2}{2m}\nabla_i^2 + \frac{1}{2}m\omega_0^2 r^2$$

$$- \beta_2 m\omega_0^2 r^2 Y_{20}(\theta, \phi)$$

$$- \mu' \hbar\omega_0 \left(l^2 - \left\langle l^2 \right\rangle_N \right)$$

$$- 2\kappa \hbar\omega_0 \vec{l} \cdot \vec{s}$$

How accurately we can describe/predict single-particle energies

1. Spherical shell model: quite accurately by fitting empirical interactions to experimental data, BUT:

- Limited to nuclei in the vicinity of doubly shell closures
- Introduces core and neglect core polarization effects

How accurately we can describe/predict single-particle energies: DFT case

$\Delta\epsilon_i = |\epsilon_i^{max} - \epsilon_i^{min}|$, where ϵ_i^{max} and ϵ_i^{min} are the largest and smallest energies of a given

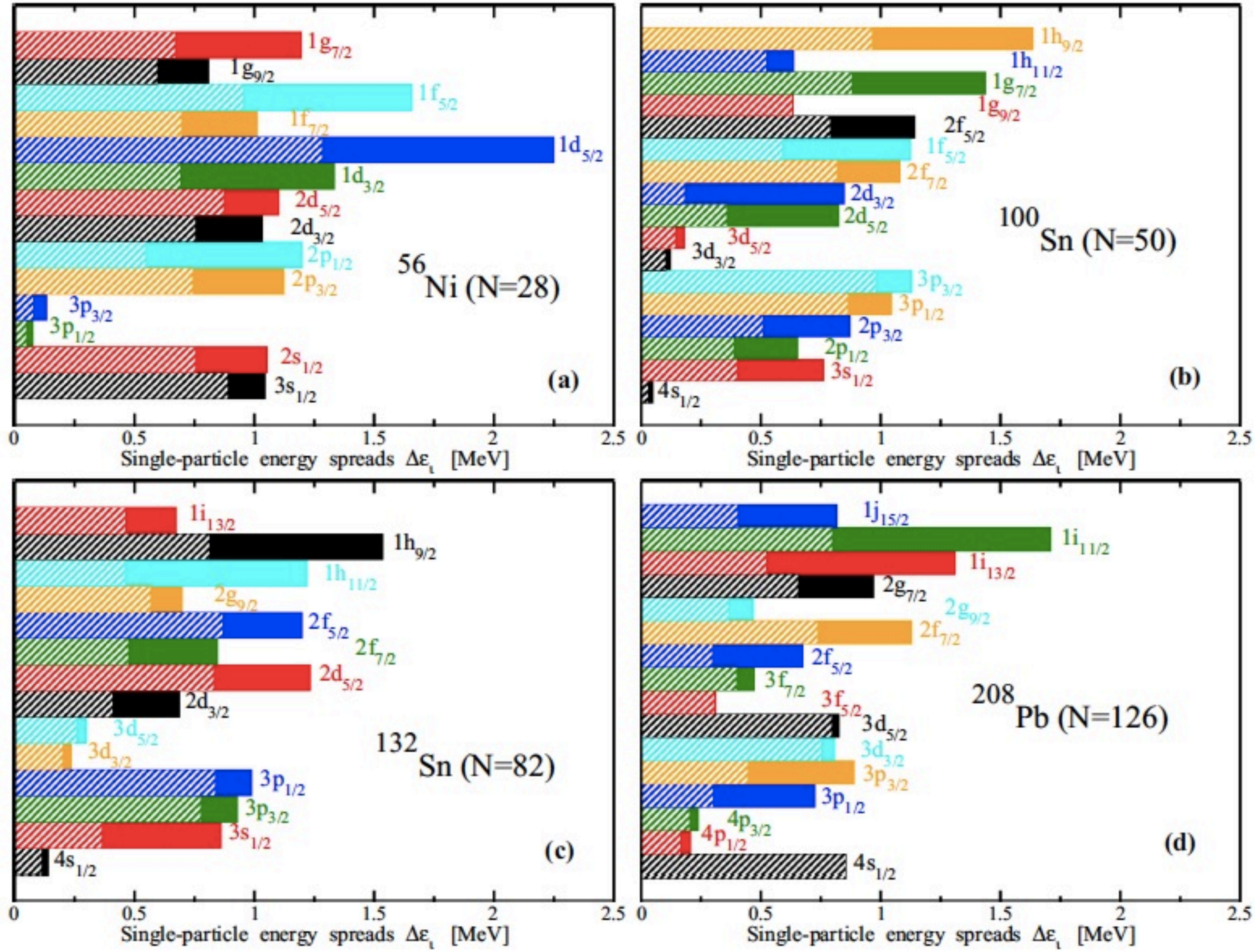

single-particle state

dashed area of bars = 4 best CEDFs of different classes

dashed+solid area of bars = 10 CEDFs

^{254}No: model dependence of the single-particle structure

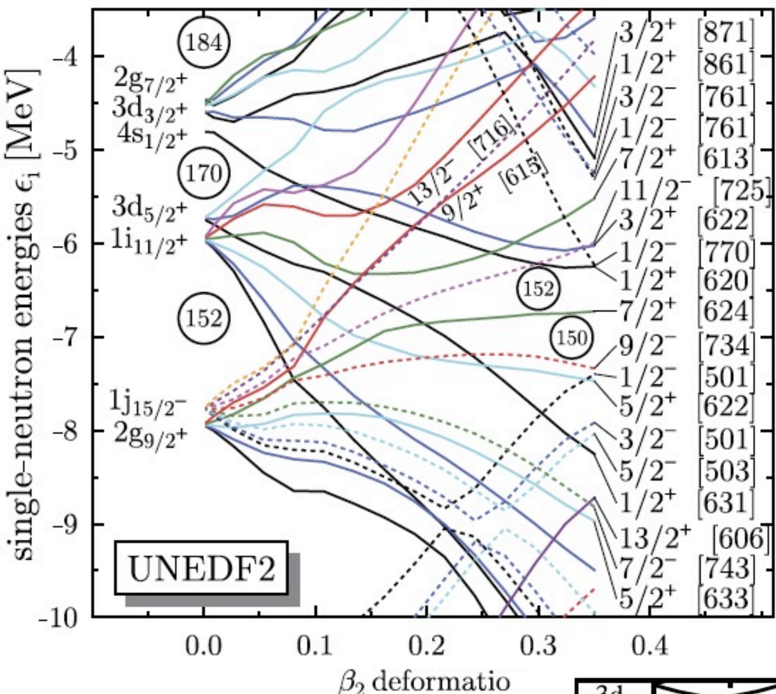

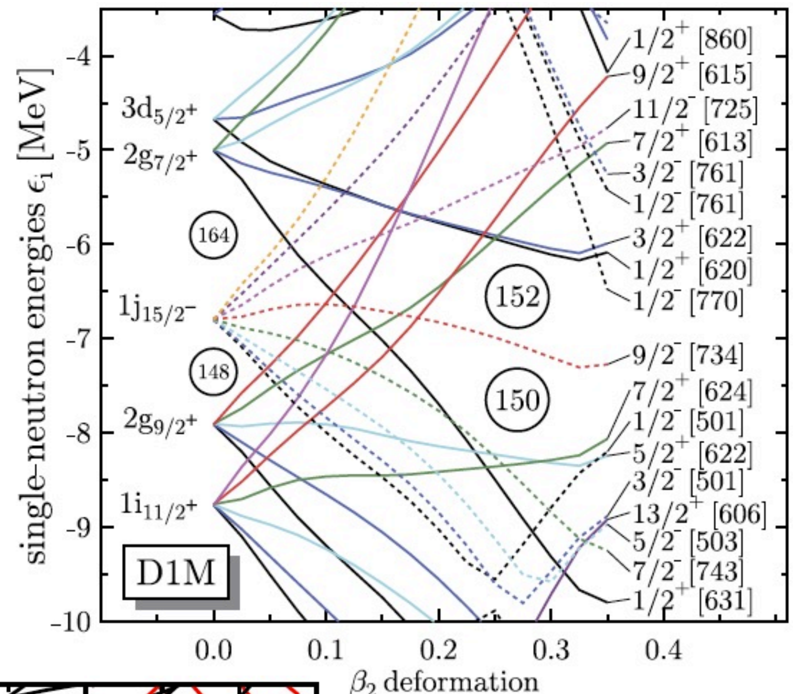

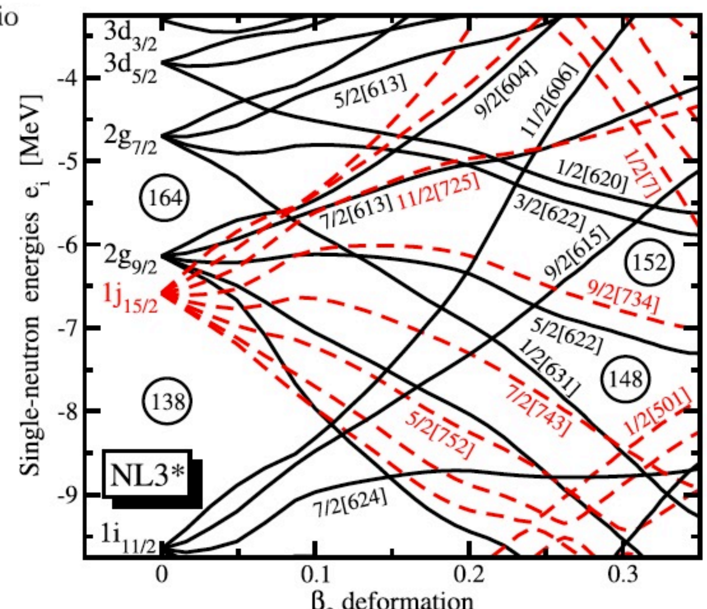

J. Dobaczewski et al, NPA 996, 388 (2015)

A global view with assessment of theoretical uncertainties

Theoretical uncertainties:

- not well defined for the regions beyond experimentally known

A. based on the set of the models which does not form statistical ensemble

B. biases of the models are not known

→ **Systematic uncertainties**

C. biases of the fitting protocols

→ **Statistical uncertainties**

Systematic uncertainties are defined by the **spreads** (the difference between maximum and minimum values of physical observable obtained with employed set of CEDF’s).

$$\Delta O(Z,N) = |O_{\max}(Z,N) - O_{\min}(Z,N)|$$

NL3*, DD-ME2, DD-MEδ, and DD-PC1 functionals

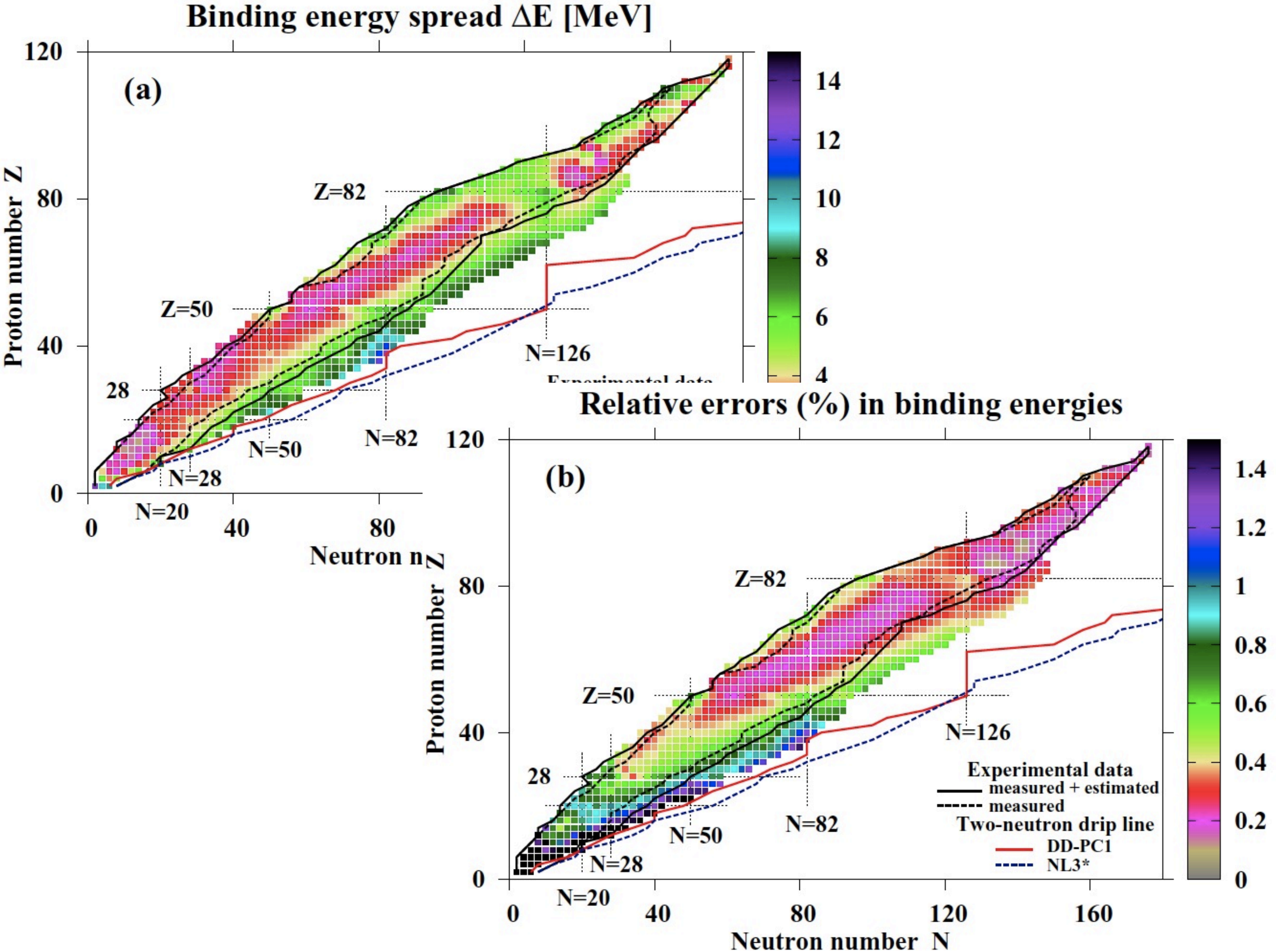

Binding energy spread ΔE [MeV]
(a)
Proton number Z
Neutron number N
Z=82
Z=50
28
N=20
N=28
N=50
N=82
N=126
Experimental data
Relative errors (%) in binding energies
(b)
Proton number Z
Neutron number N
Z=82
Z=50
28
N=20
N=28
N=50
N=82
N=126
Experimental data
measured + estimated
measured
Two-neutron drip line
DD-PC1
NL3*

Proton β_2-deformation

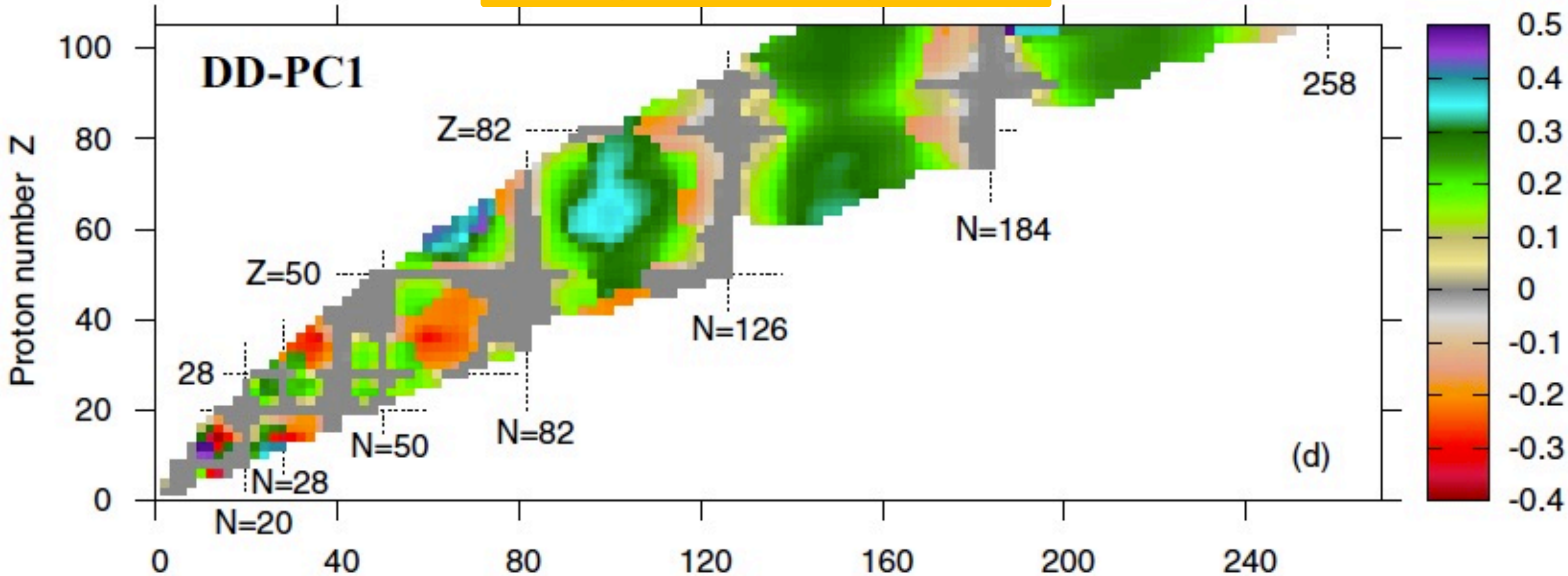

Proton hexadecapole β_4-deformation

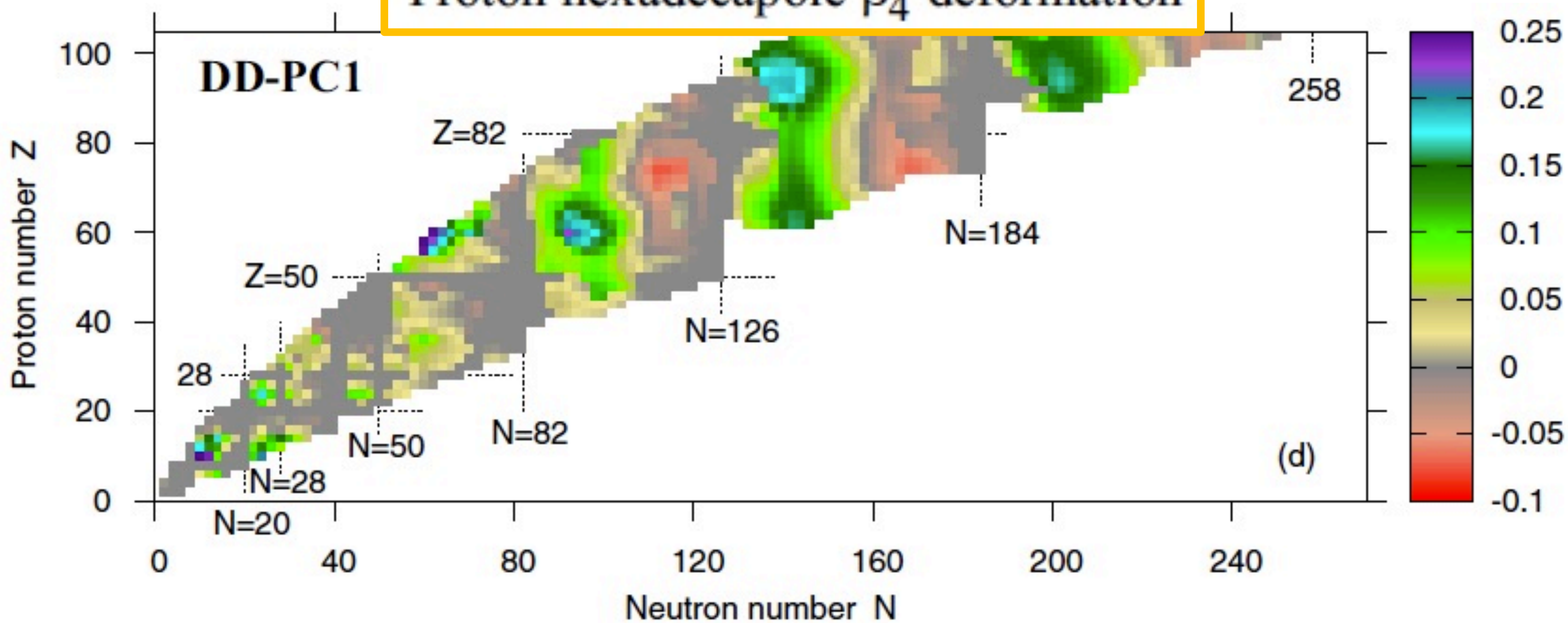

S. Agbemava, AA, D, Ray, P.Ring, PRC **89**, 054320 (2014)

Deformations of the ground states in actinides states

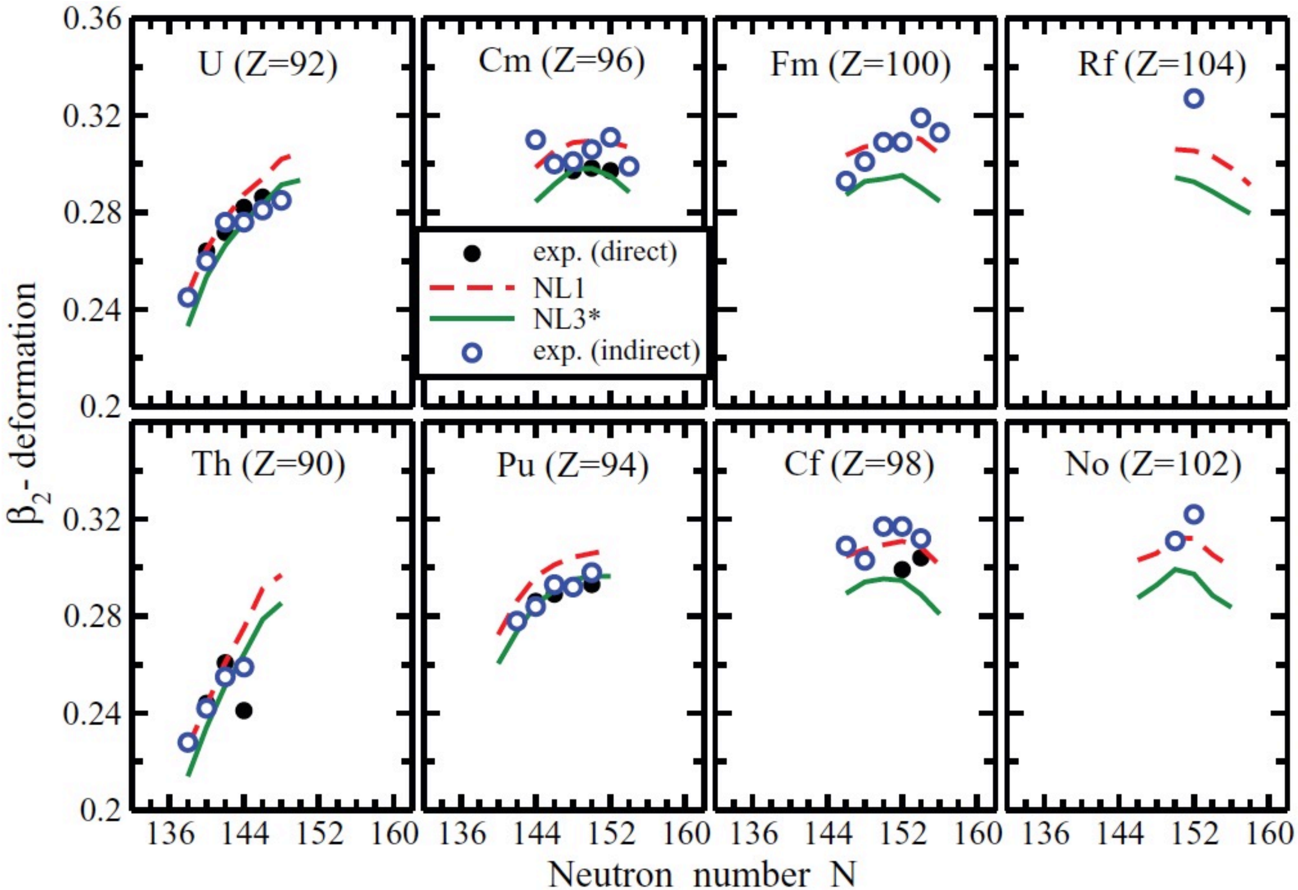

Experiment:
Direct = Coulomb excitations and lifetime measurements
Indirect = Grodzins relation

AA and O.Abdurazakov, PRC 88, 014320 (2013)

$$\beta_2 = Q_{20} / \left(\sqrt{\frac{16\pi}{5}} \frac{3}{4\pi} A R_0^2 \right)$$

Note: including higher powers of β_2 yields the values of β_2 that are ~10% lower

Proton quadrupole deformation spread $\Delta\beta_2$

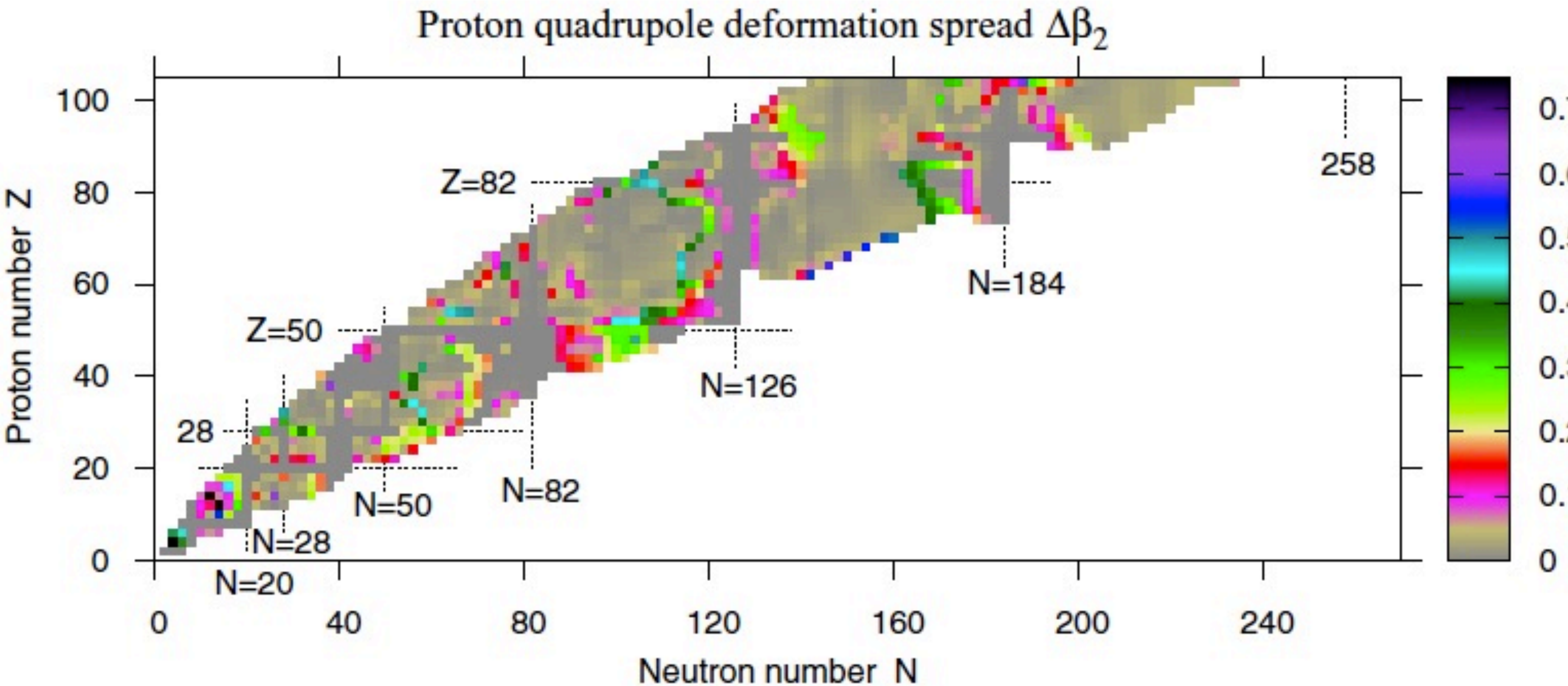

Theoretical uncertainties are most pronounced for transitional nuclei (due to soft potential energy surfaces) and in the regions of transition between prolate and oblate shapes. Details depend on the description of single-particle states

S. Agbemava, AA, D, Ray, P.Ring, PRC **89**, 054320 (2014)

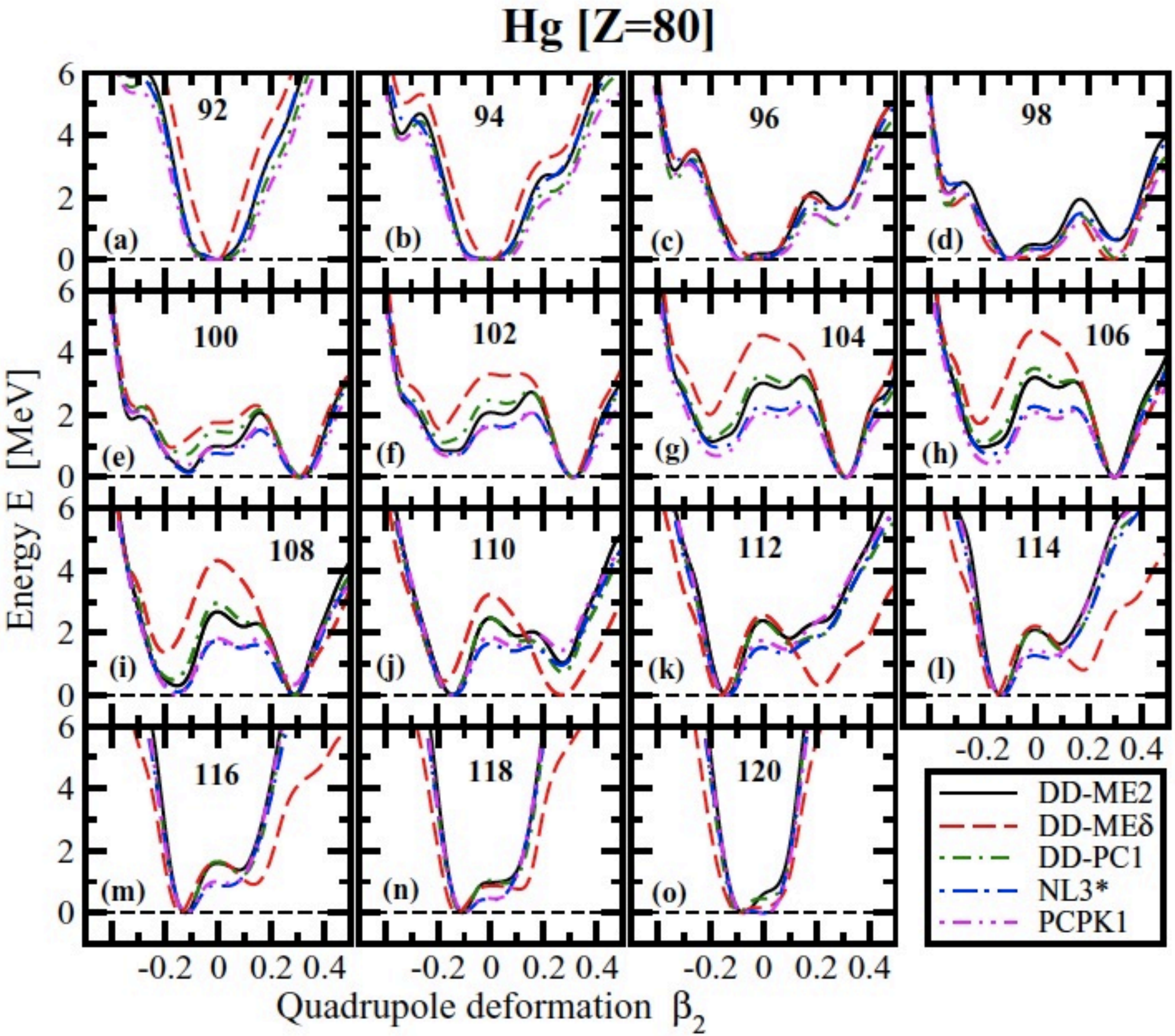

Hg [Z=80]
92
94
96
98
100
102
104
106
108
110
112
114
116
118
120
(a)
(b)
(c)
(d)
(e)
(f)
(g)
(h)
(i)
(j)
(k)
(l)
(m)
(n)
(o)
Energy E [MeV]
Quadrupole deformation β2
DD-ME2
DD-MEδ
DD-PC1
NL3*
PCPK1

Proton hexadecapole deformation spread $\Delta\beta_4$

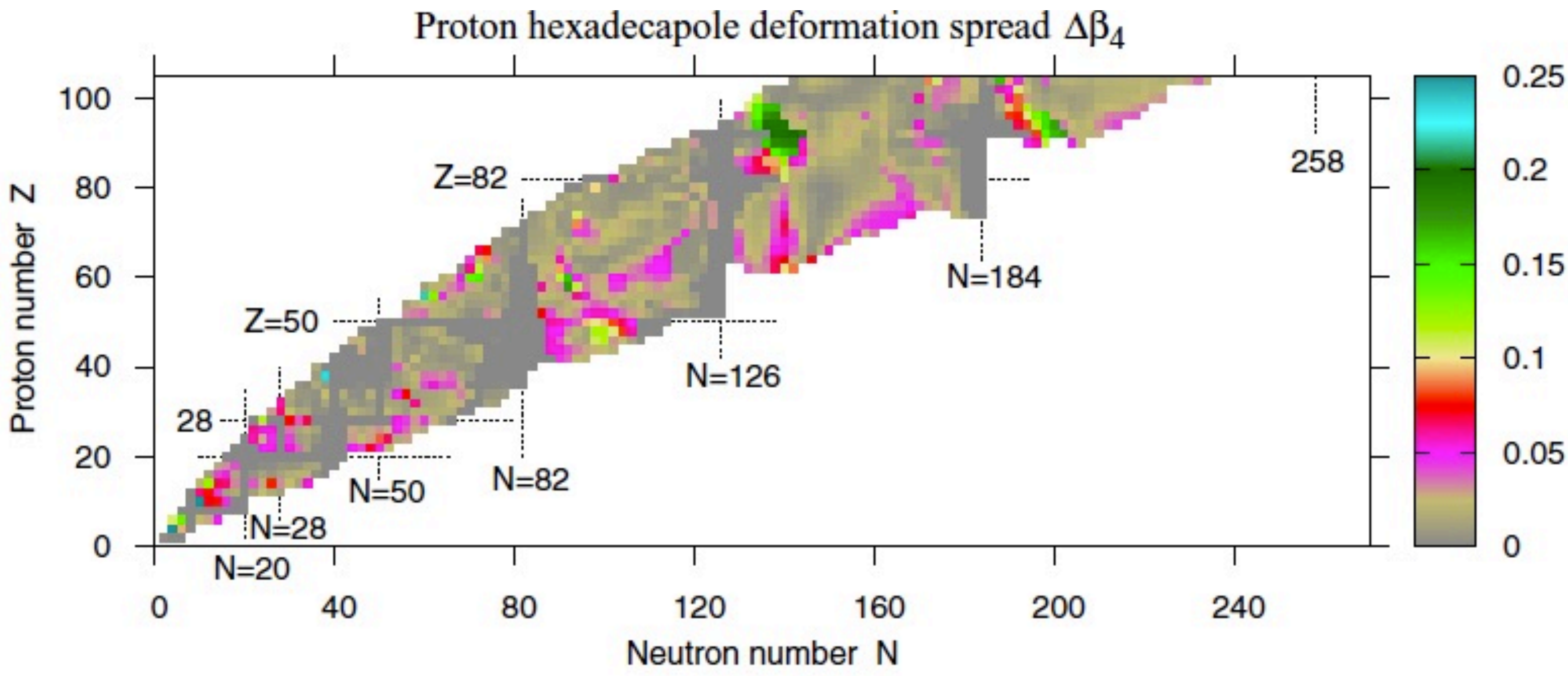

Theoretical uncertainties are most pronounced for transitional nuclei (due to soft potential energy surfaces) and in the regions of transition between prolate and oblate shapes. Details depend of the description of single-particle states

S. Agbemava, AA, D, Ray, P.Ring, PRC **89**, 054320 (2014)

Isovector $\beta_2^{IV} = \beta_2(\nu) - \beta_2(\pi)$ deformations

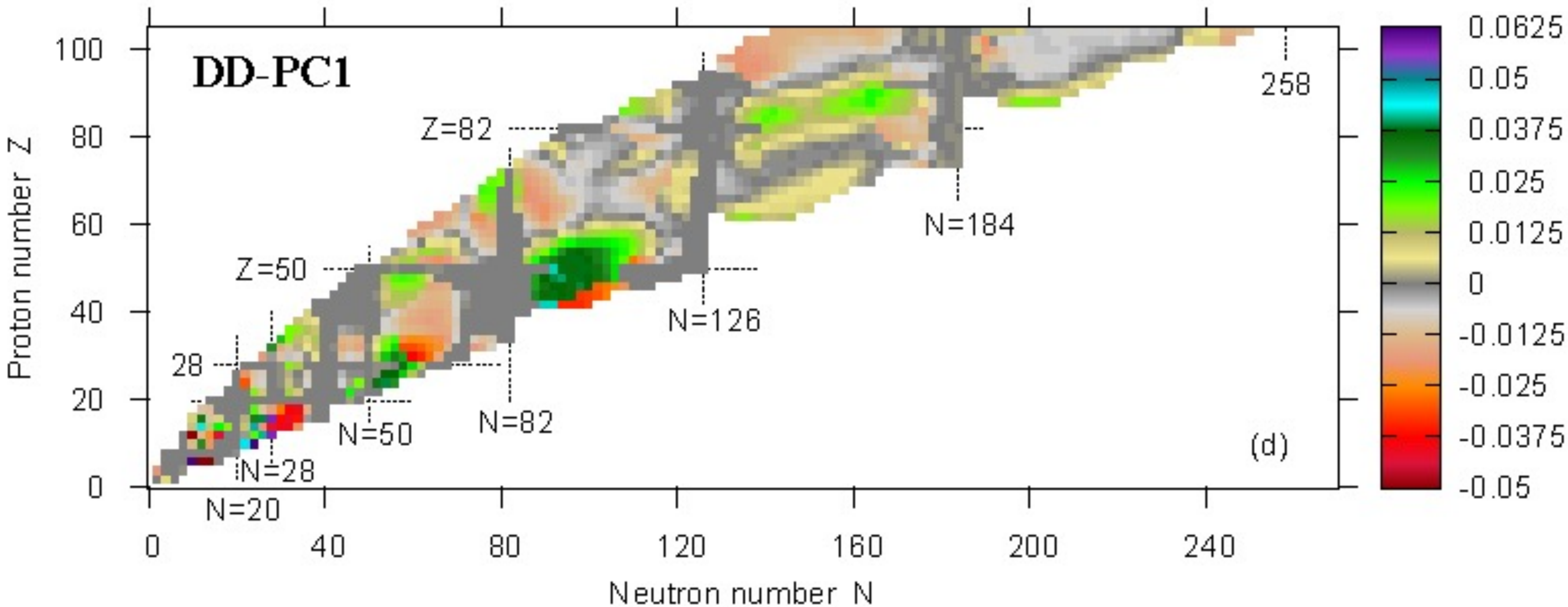

S. Agbemava, AA, D, Ray, P.Ring, PRC **89**, 054320 (2014)

CDFT: Neutron deformation is larger than proton one in ~ 2/3 of nuclei, in the rest of deformed nuclei the situation is opposite

Skyrme DFT: Neutron deformation is smaller than proton one in majority of nuclei.

Isovector deformation is typically smaller in CDFT → **mic+mac model,** which assumes the same deformation for protons and neutrons, is **is better justified in CDFT than in Skyrme DFT**.

DD-MEY versus non-relativistic UNEDF* functionals

Fitting protocol of DD-MEY functional

- Isospin-dependent pairing interaction from S. Teeti and AA, PRC 103, 034310 (2021).
- Fitting only to binding energies and charge radii of 12 spherical nuclei.

Functional/ Observables	DD-MEX	DD-MEY	UNEDF 0	UNEDF 1	UNEDF2
ΔE_{rms} [MeV]	**1.790**	**1.719**	1.428	1.912	1.950
K_0 [MeV]	**306.7**	**265.8**	230.0	220.0	239.930
J [MeV]	32.431	32.778	30.543	28.987	29.131
L [MeV]	53.526	51.831	45.080	40.005	40.0
R_{skin}(Ca-48) [fm]	**0.185**	**0.189**			
R_{skin}(Pb-208) [fm]	**0.198**	**0.198**			0.167

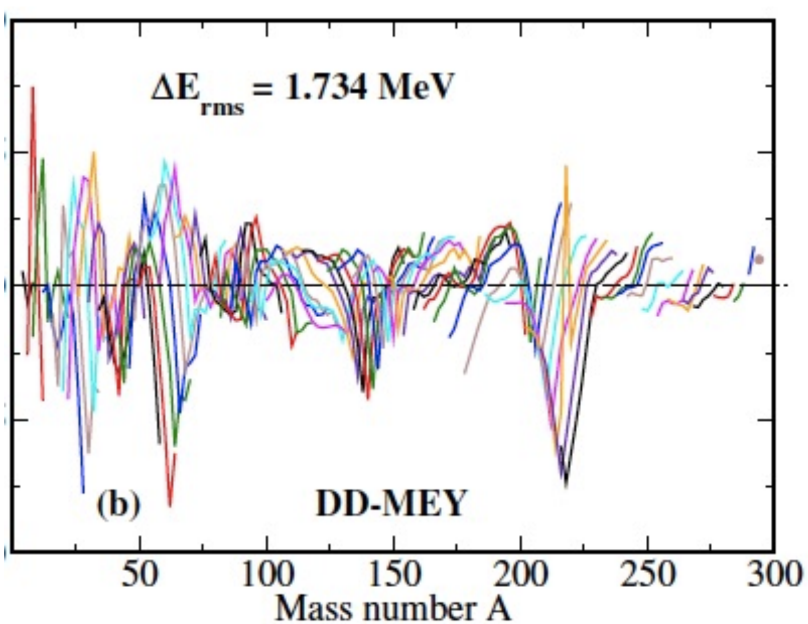

Empirical range of nuclear matter properties

K_0 : 190 – 270
J : 25 – 35
L_0 : 25 – 115

Fitting protocol of UNEDF2 contains 47 deformed and 28 spherical nuclei, M. Kortelainen et al, PRC 82, 024313 (2010).

A. Taninah and AA, submitted to PRC, 2022

Differential charge radii: when they reveal a deformation

Charge radii $r_{ch} = \sqrt{< r^2 >_p + 0.64}$ fm

Differential mean square charge radius

$$\boxed{\begin{aligned} \delta \left\langle r^2 \right\rangle_p^{N,N'} &= \left\langle r^2 \right\rangle_p (N) - \left\langle r^2 \right\rangle_p (N') = \\ &= r^2_{ch}(N) - r^2_{ch}(N') \end{aligned}}$$

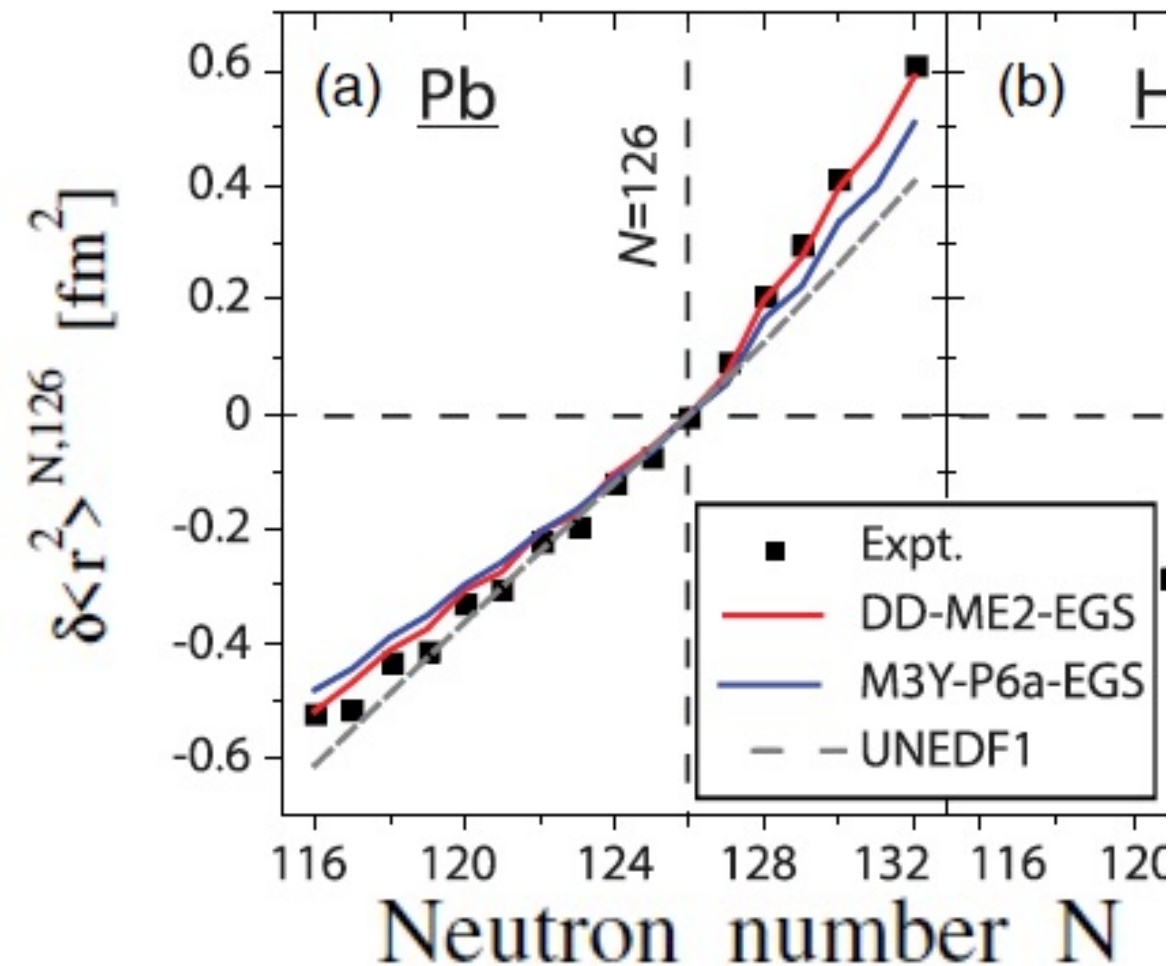

T. Day Goodacre, AA, et al,
PRL 126, 032502 (2021)

Hg [Z=80]

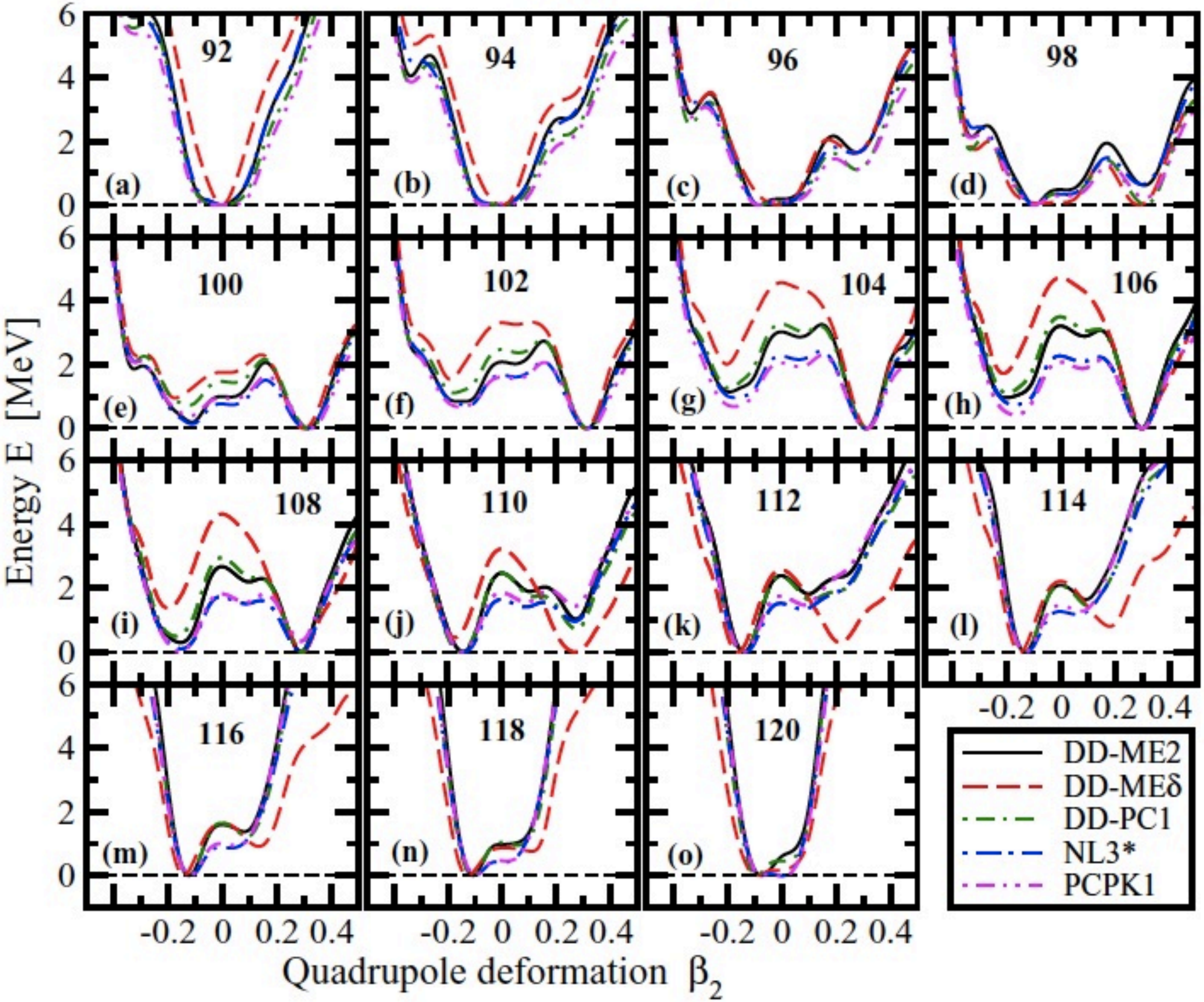

U.C.Perera, AA and P.Ring,
PRC 104, 064313 (2021)

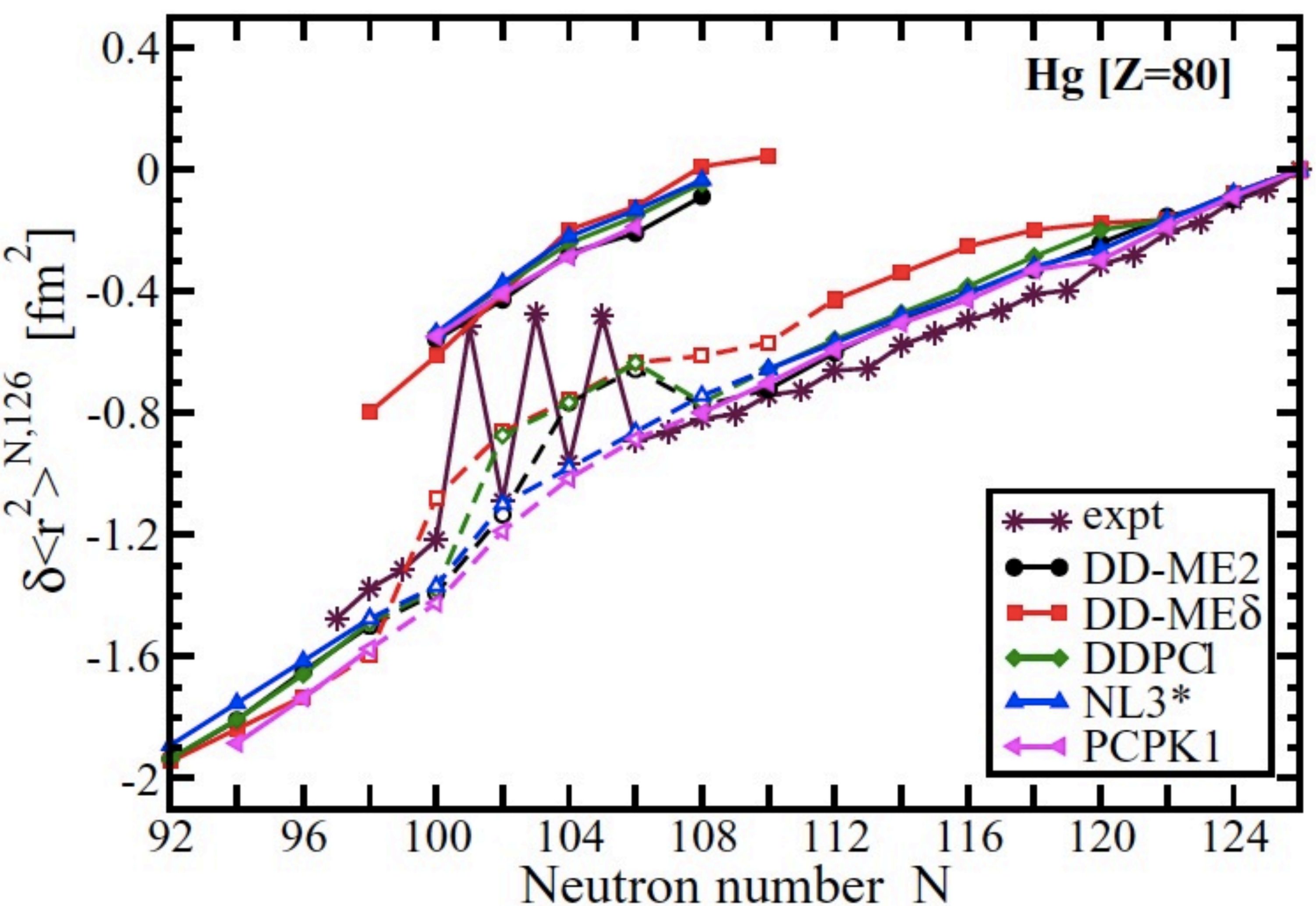
Hg [Z=80]
$\delta\langle r^2\rangle^{N,126}$ [fm^2]
Neutron number N
0.4
0
-0.4
-0.8
-1.2
-1.6
-2
92
96
100
104
108
112
116
120
124
expt
DD-ME2
DD-MEδ
DDPCl
NL3*
PCPK1

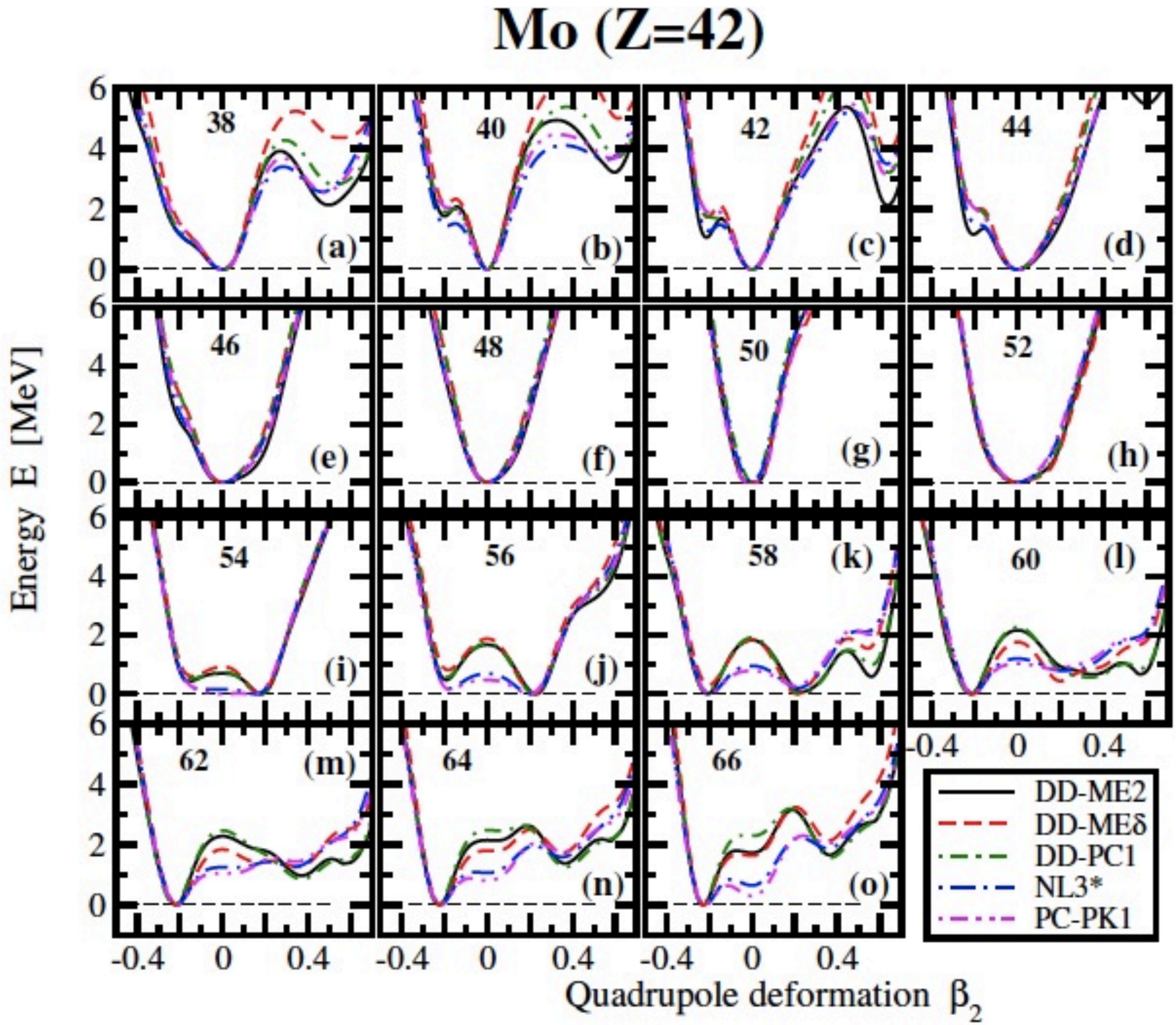
Mo (Z=42)
Energy E [MeV]
Quadrupole deformation β_2
38 (a)
40 (b)
42 (c)
44 (d)
46 (e)
48 (f)
50 (g)
52 (h)
54 (i)
56 (j)
58 (k)
60 (l)
62 (m)
64 (n)
66 (o)
DD-ME2
DD-MEδ
DD-PC1
NL3*
PC-PK1

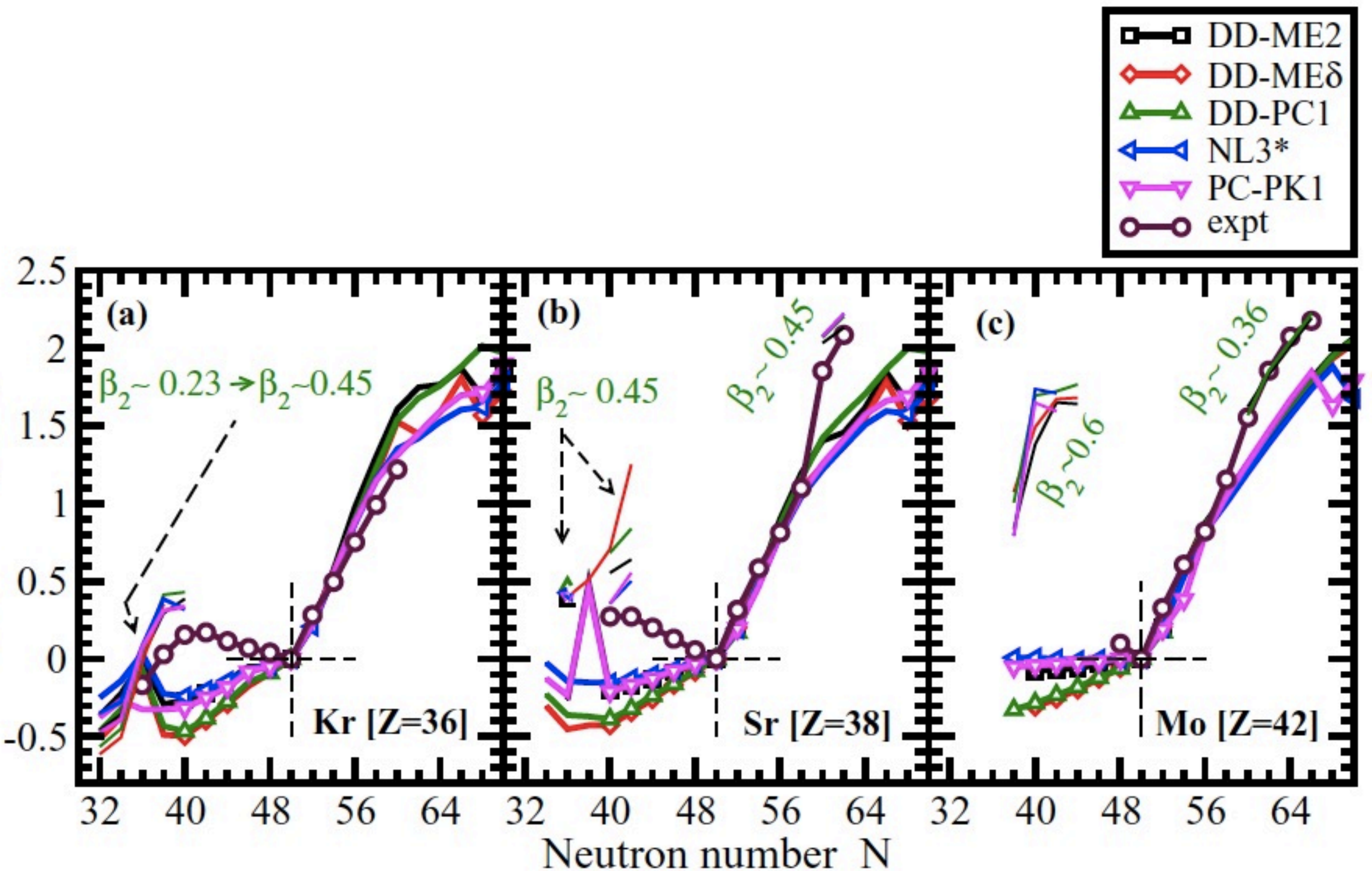

DD-ME2
DD-MEδ
DD-PC1
NL3*
PC-PK1
expt
(a)
(b)
(c)
β2~ 0.23 → β2~0.45
β2~ 0.45
β2~ 0.45
β2~0.6
β2~ 0.36
Kr [Z=36]
Sr [Z=38]
Mo [Z=42]
δ<r2>N,50 [fm2]
Neutron number N

Rotation in nuclei: a clear signal of deformation.

A.V.Afanasjev, P.Ring, J. Konig, PRC 60 (1999) R051303, Nucl. Phys. A 676(2000) 196

Cranked Relativistic Hartree-Bogoliubov Theory

The CRHB equations for the fermions in the rotating frame in the one-dimensional cranking approximation

$$\begin{pmatrix} h_D - \lambda - \Omega_x \hat{J}_x & \hat{\Delta} \\ -\hat{\Delta}^* & -h_D^* + \lambda + \Omega_x \hat{J}_x \end{pmatrix} \begin{pmatrix} U_k \\ V_k \end{pmatrix} = E_k \begin{pmatrix} U_k \\ V_k \end{pmatrix}$$

Coriolis term

Klein-Gordon equations

$$\begin{aligned} \left\{-\Delta - (\Omega_x \hat{L}_x)^2 + m_\sigma^2\right\} \sigma(\boldsymbol{r}) &= -g_\sigma \rho_s(\boldsymbol{r}) - g_2 \sigma^2(\boldsymbol{r}) - g_3 \sigma^3(\boldsymbol{r}) \\ \left\{-\Delta - (\Omega_x \hat{L}_x)^2 + m_\omega^2\right\} \omega_0(\boldsymbol{r}) &= g_\omega \rho_v^{is}(\boldsymbol{r}) \\ \left\{-\Delta - (\Omega_x (\hat{L}_x + \hat{S}_x))^2 + m_\omega^2\right\} \boldsymbol{\omega}(\boldsymbol{r}) &= g_\omega \boldsymbol{j}^{is}(\boldsymbol{r}) \end{aligned}$$

Space-like components of vector mesons

currents

Important in rotating nuclei: give ~ 20-30% contr. to moments of inertia

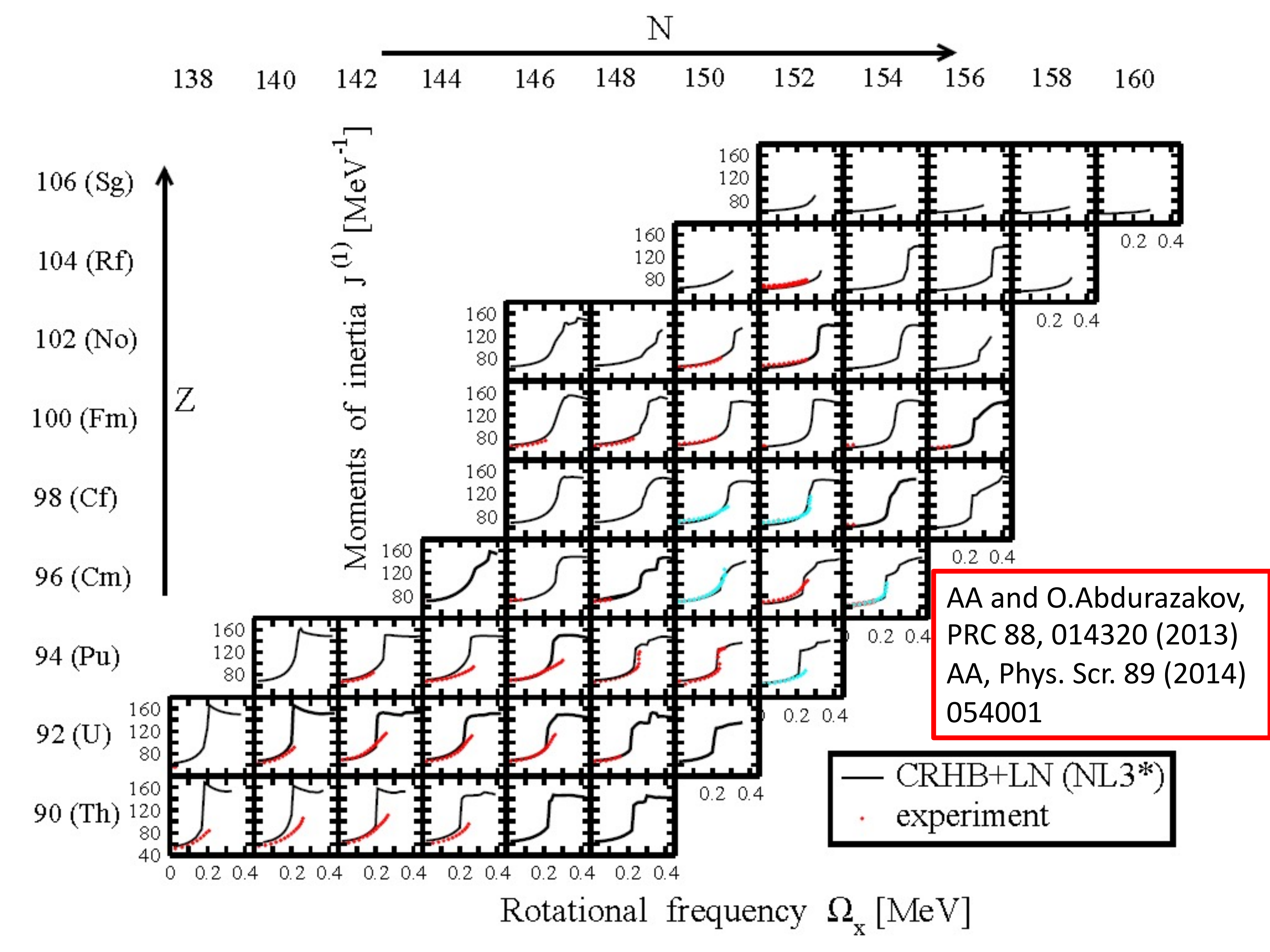
N
138
140
142
144
146
148
150
152
154
156
158
160
Z
106 (Sg)
104 (Rf)
102 (No)
100 (Fm)
98 (Cf)
96 (Cm)
94 (Pu)
92 (U)
90 (Th)
Moments of inertia $J^{(1)}$ [MeV^{-1}]
Rotational frequency Ω_x [MeV]
CRHB+LN (NL3*)
experiment
AA and O.Abdurazakov, PRC 88, 014320 (2013)
AA, Phys. Scr. 89 (2014) 054001

Survey of octupole deformation.

Landscape of pear-shaped even-even nuclei

Model multiplicity m(Z,N) = number of models predicting non-zero octupole deformation in the nucleus with (Z,N)

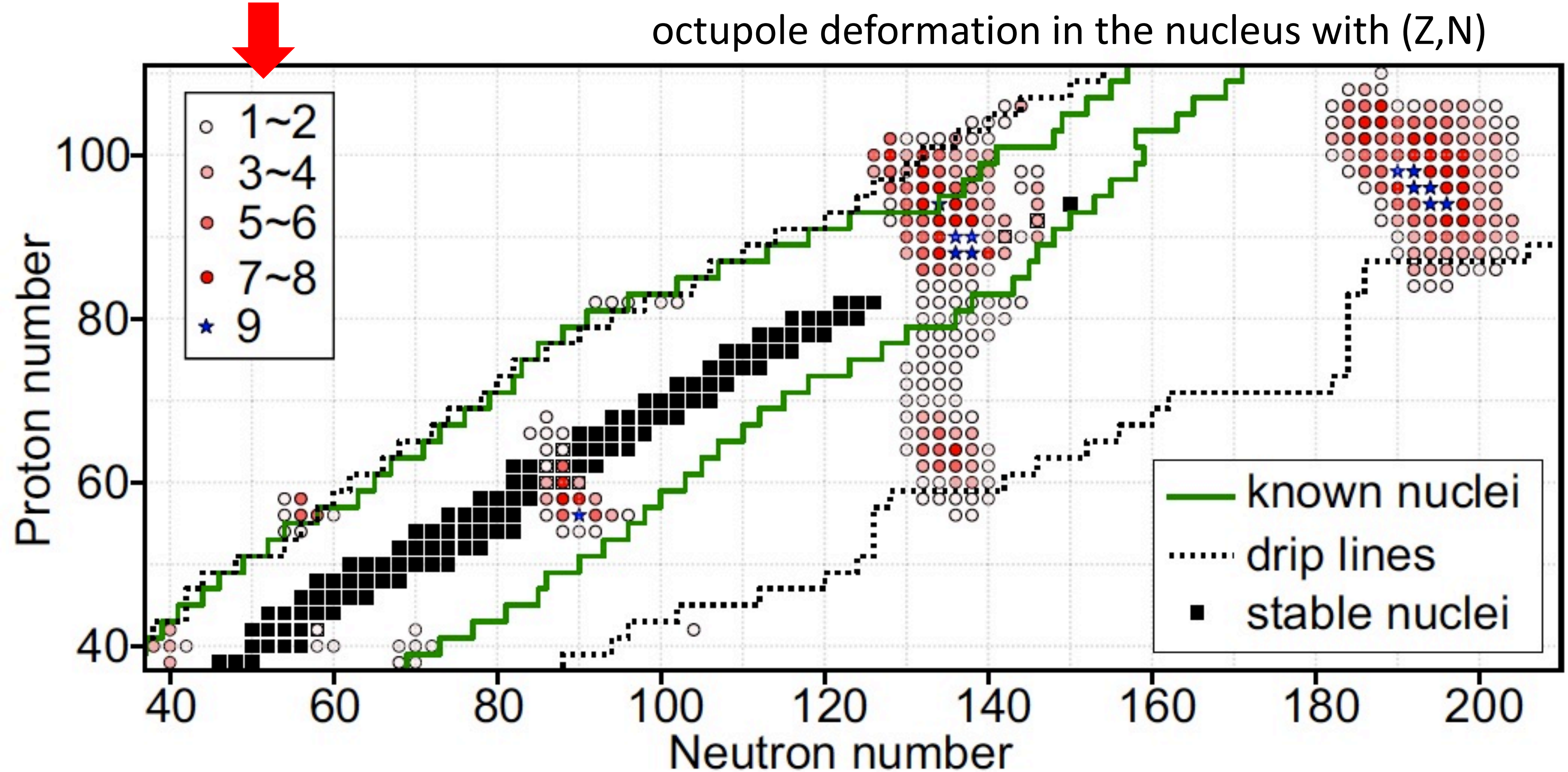

- the RHB calculations with 4 CEDFs
- Skyrme HFB calculations with 5 EDFs

Y. Cao et al, AA, PRC 102, 024311 (2020)

CDFT vs Skyrme DFT predictions for octupole deformed nuclei

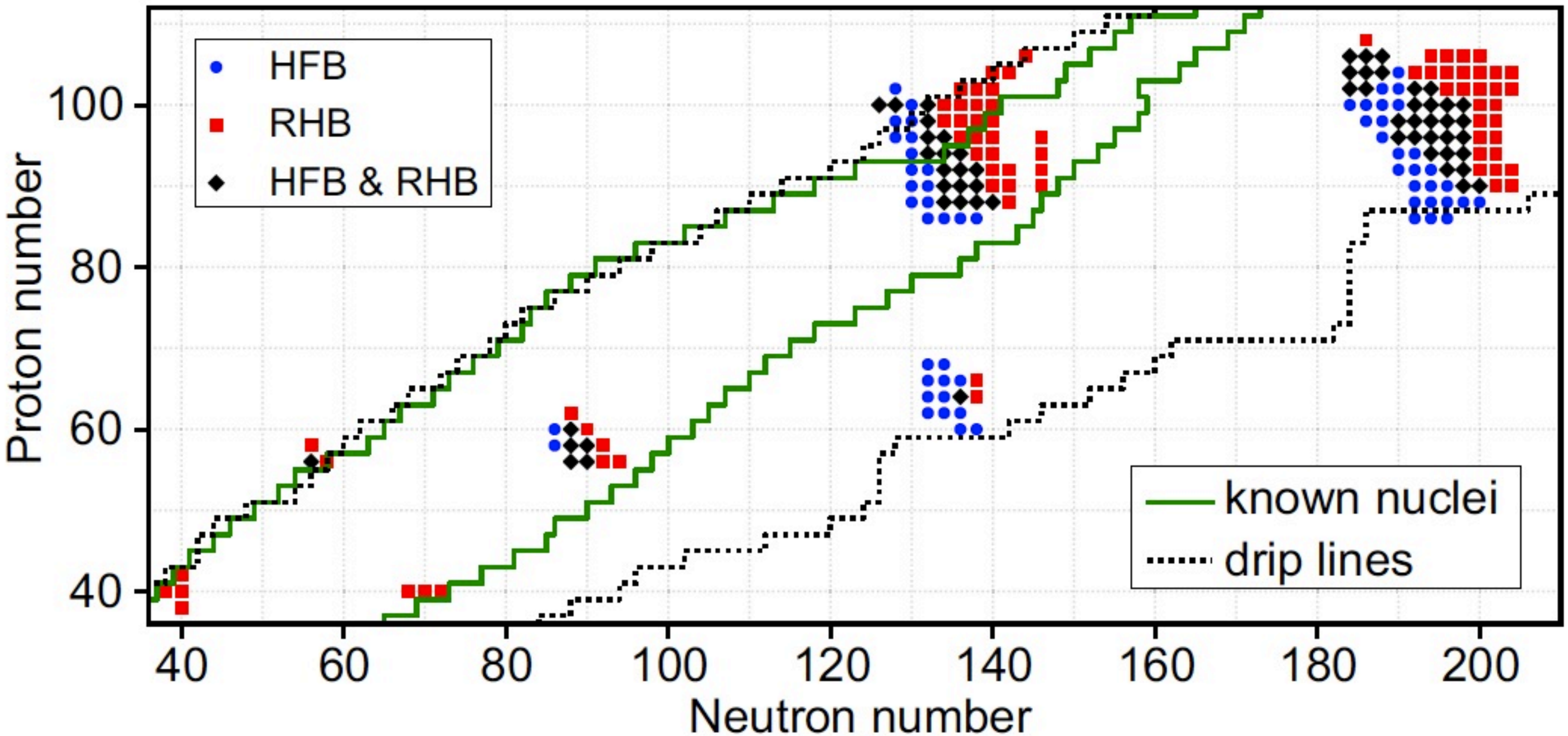

A shift in the position of octupole deformed regions (by two to four neutron numbers) is seen when comparing the results of CDFT and SDFT calculations. It comes from the differences In the underlying single-particle structure

Y. Cao et al, AA, PRC 102, 024311 (2020)

Extreme dependence of the predictions for octupole deformation on model/functional

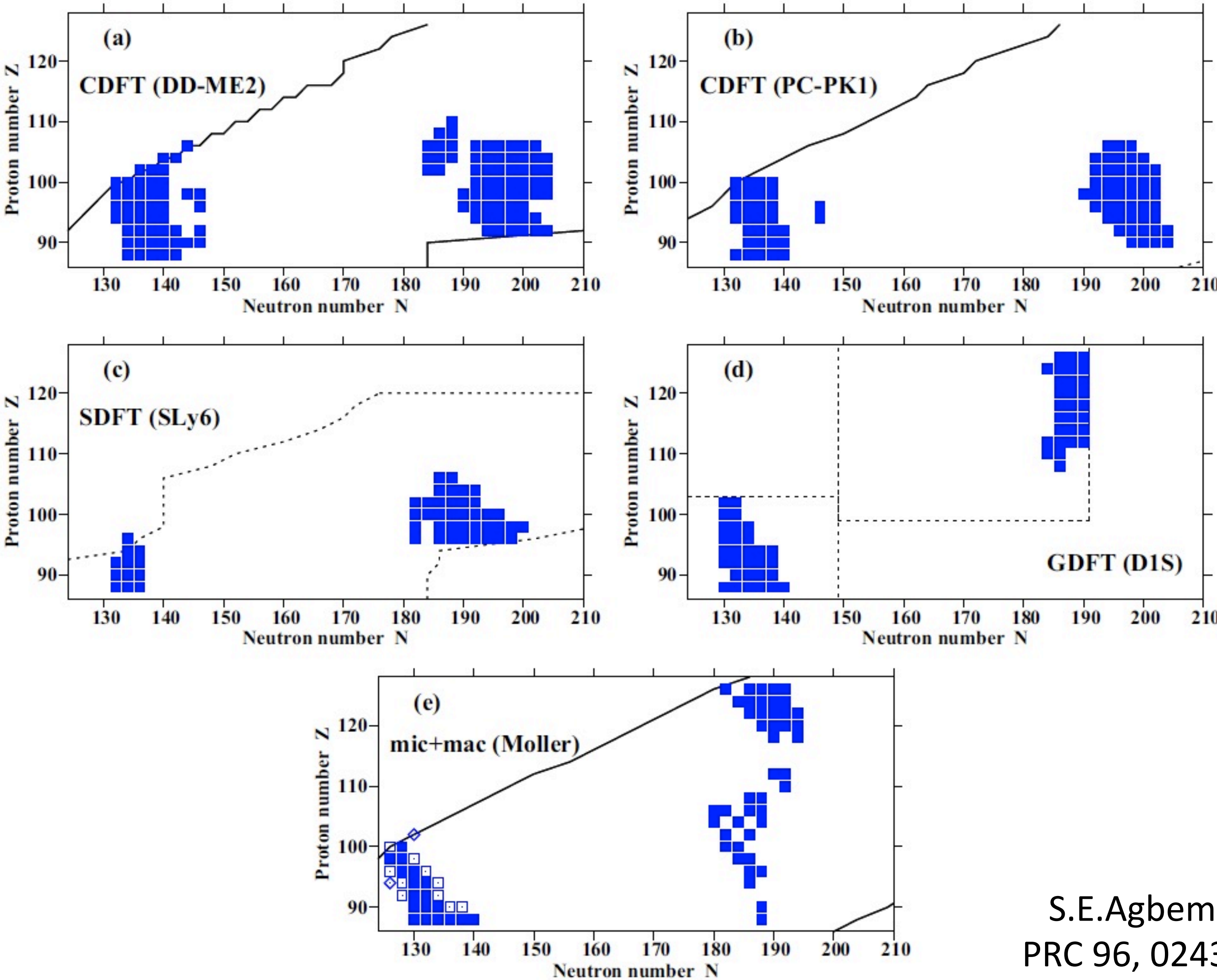

S.E.Agbemava, AA,
PRC 96, 024301 (2017)

Factors affecting the predictions of octupole deformed nuclei

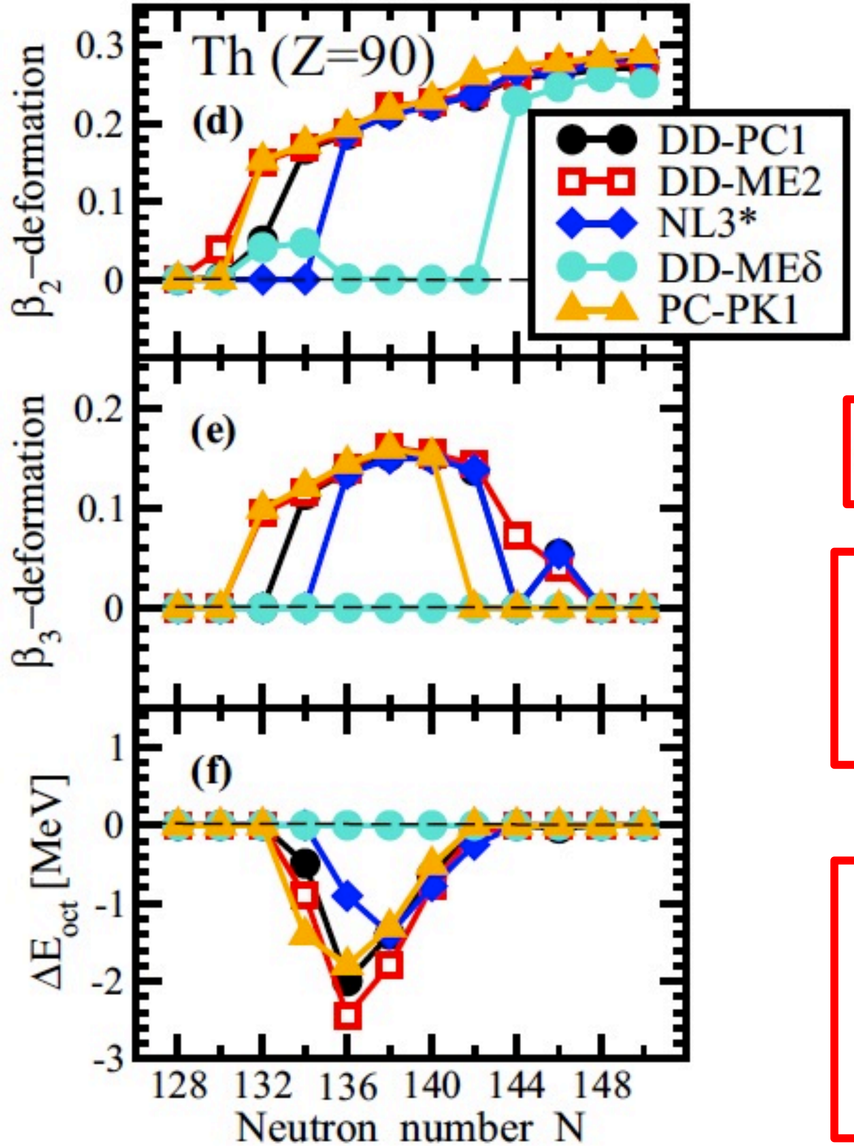

S.E.Agbemava, AA,
PRC 93, 044304 (2016)

$$\Delta E_{\text{oct}} = E^{\text{oct}}(\beta_2, \beta_3) - E^{\text{quad}}(\beta_2', \beta_3' = 0)$$

The differences in the underlying single-particle structure are responsible for the differences in predictions

The non-existence of the octupole deformation in the DD-MEδ functional is most likely due to too large Z=92 spherical shell gap

Factors affecting the predictions of octupole deformed nuclei: pairing

$$V(\boldsymbol{r}_1, \boldsymbol{r}_2, \boldsymbol{r}_1', \boldsymbol{r}_2') = \\ = -f\, G \delta(\boldsymbol{R} - \boldsymbol{R}') P(r) P(r') \frac{1}{2}(1 - P^{\sigma})$$

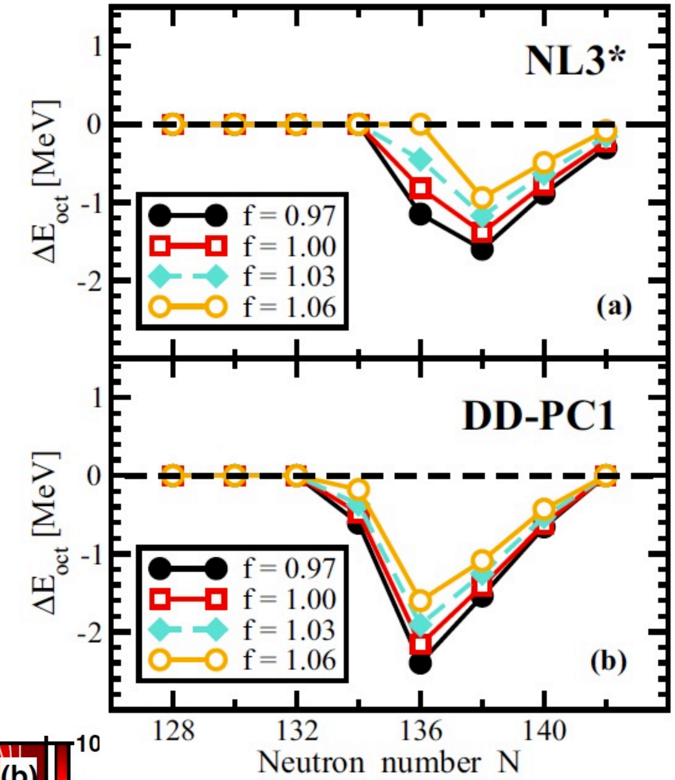

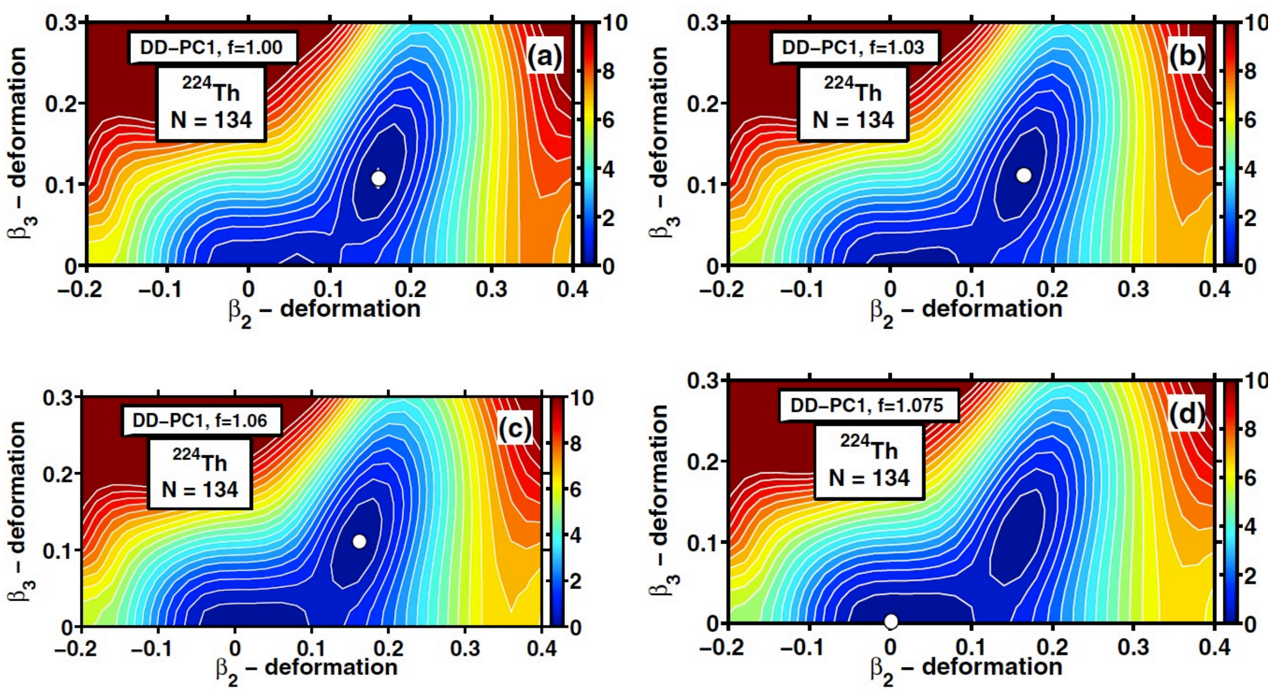

S.E.Agbemava, AA,
PRC 93, 044304 (2016)

The challenges of the Sm isotopes

$$\Delta E_{\rm oct} = E^{\rm oct}(\beta_2,\beta_3) - E^{\rm quad}(\beta_2',\beta_3'=0)$$

our RHB: only ^{150}Sm ΔE_{oct}=0.25 MeV (DD-PC1)
ΔE_{oct}=0.09 MeV (NL3*)

S.E.Agbemava, AA,
PRC 93, 044304 (2016)

RMF+BCS (PK1) : ^{146,148,150,152}Sm [PRC 81, 034302 (2010)]
maximum ΔE_{oct}=1.36 MeV in ^{150}Sm
not supported by experimental data

RHB (DD-PC1) : ^{148,150,156}Sm [PRC 89, 024312 (2014)]
extremely soft PES in octupole direction

Mic+mac
[Woods-Saxon potential, PRC 45, 2026 (1992)] no octupole def
[folded Yukawa, ADNDT 94 758 (2008)] ΔE_{oct}=0.02 MeV in ^{150}Sm

Gogny DFT: HF+BCS(D1S) ^{148,150}Sm, NPA 545, 589 (1992).
HFB(D1S and D1M) ^{150}Sm, ΔE_{oct}=0.204 and 0.043 MeV, PRC 86, 034336 (2012)].

!!! No clear experimental fingerprints of static octupole deformation

The challenge of superheavy nuclei

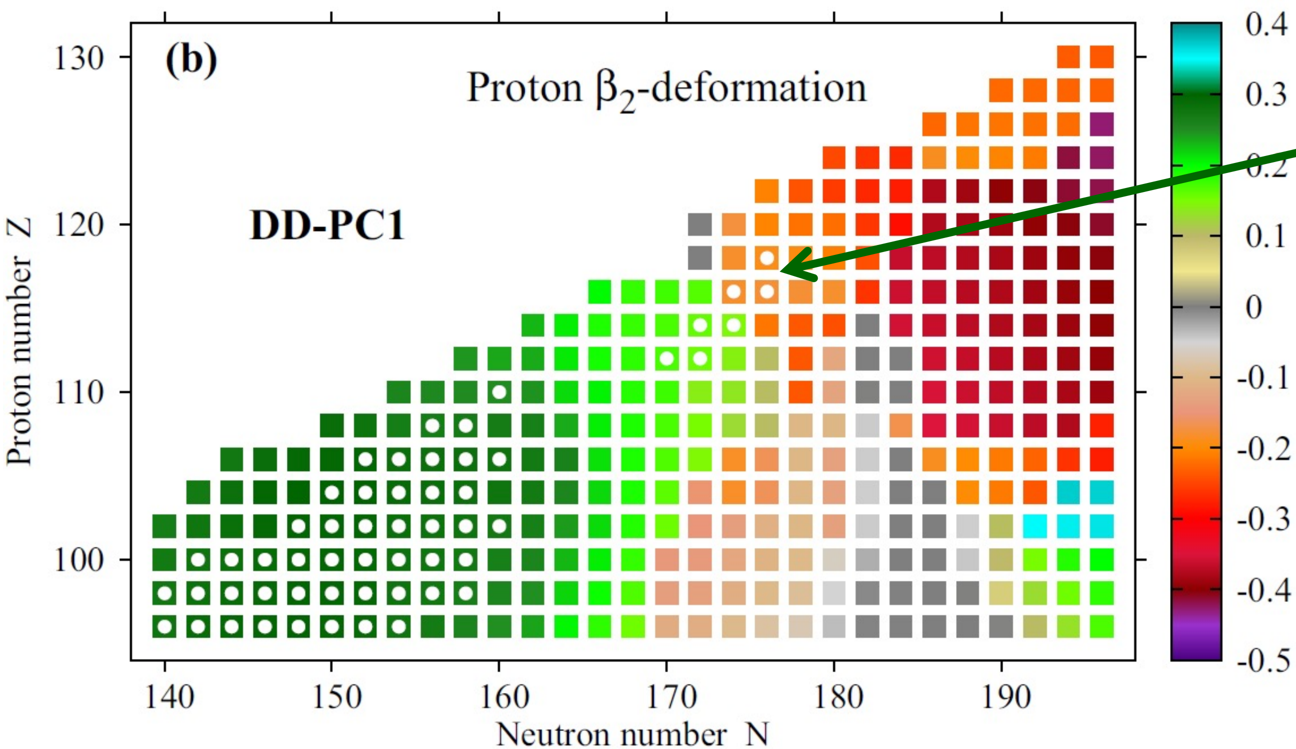

DD-PC1:
Experimental Z=116, 118 nuclei are oblate

PC-PK1:
Experimental Z=118 nucleus is spherical

Other experimental SHE are prolate

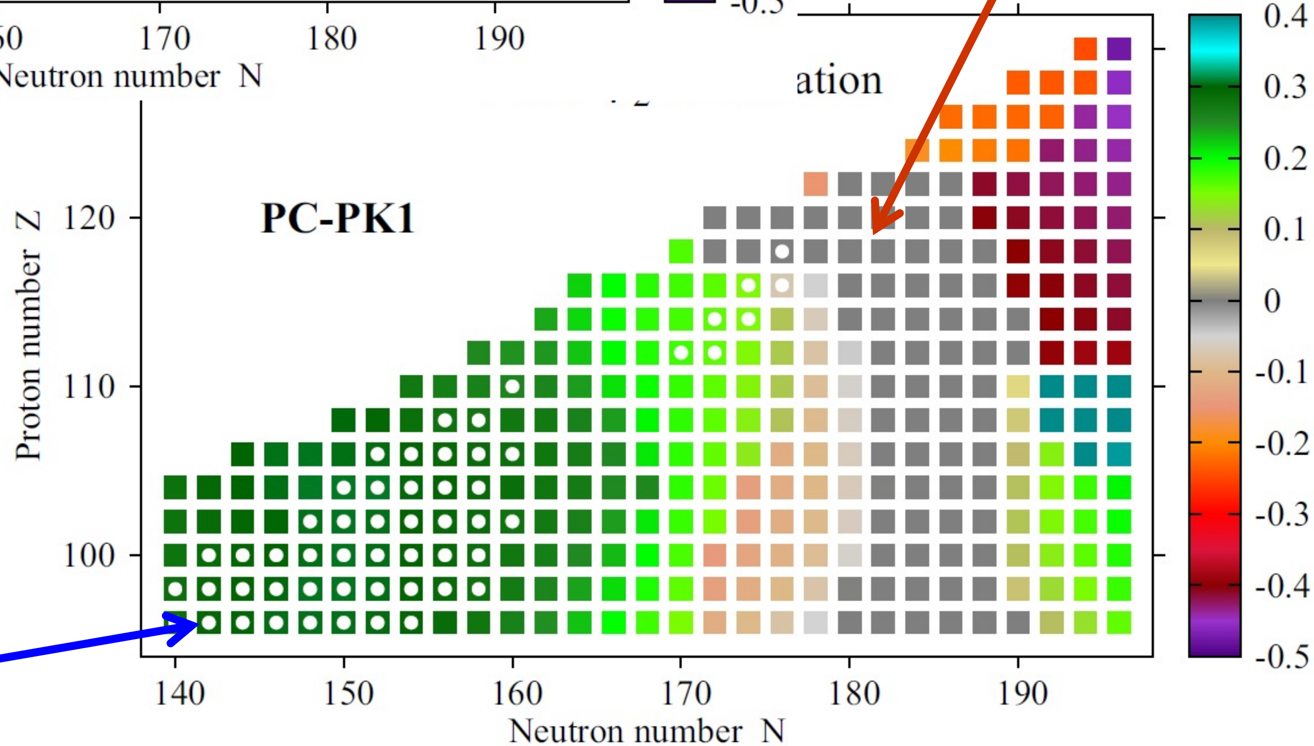

Open circles – experimentally observed nuclei

S. Agbemava et al, PRC **92**, 054310 (2015)

Impact of the correlations beyond mean field on the ground states and saddle points of superheavy nuclei

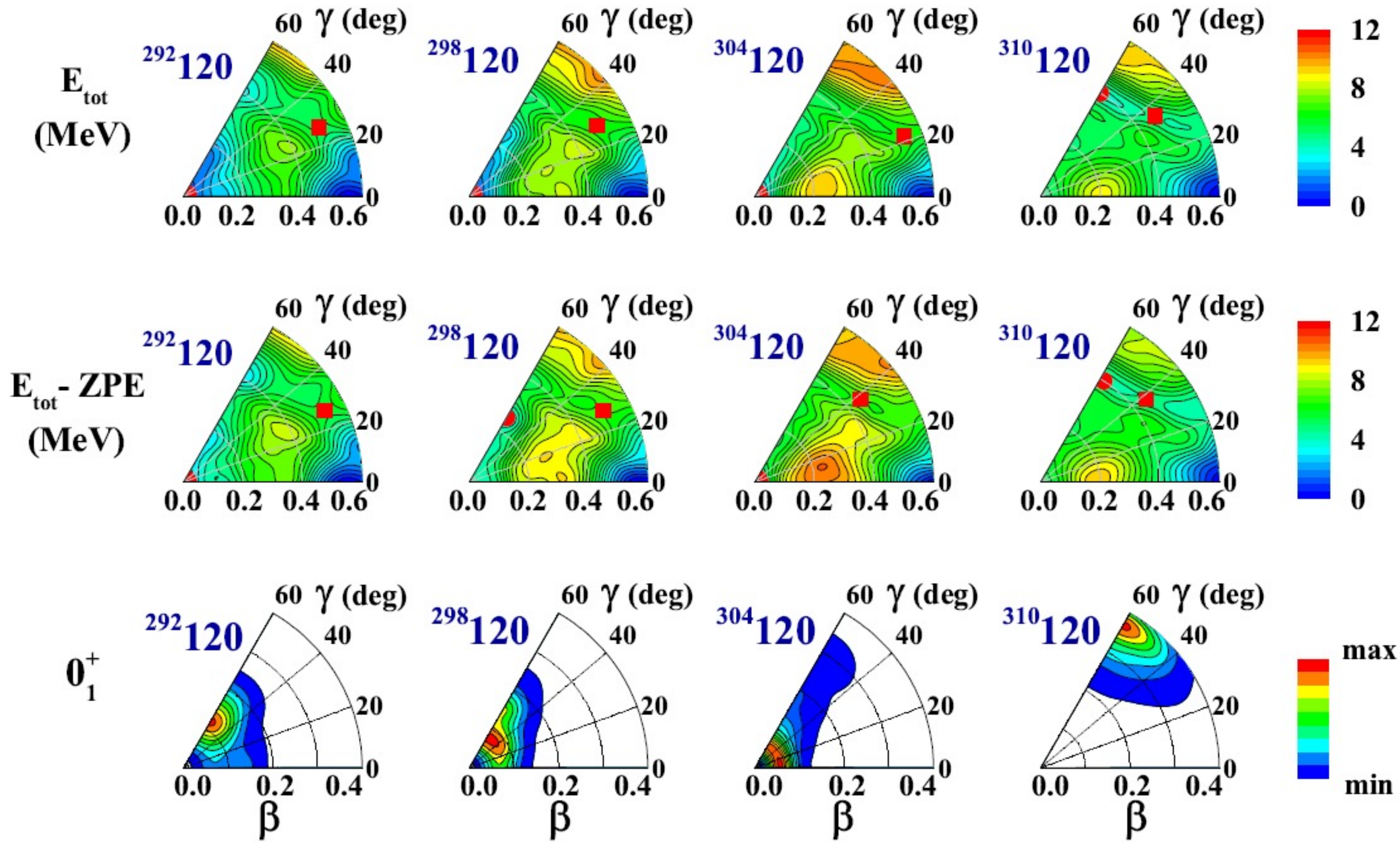

The energy difference between the neighboring contour lines is 0.5 MeV.

Impact of the correlations beyond mean field on the ground states of superheavy nuclei

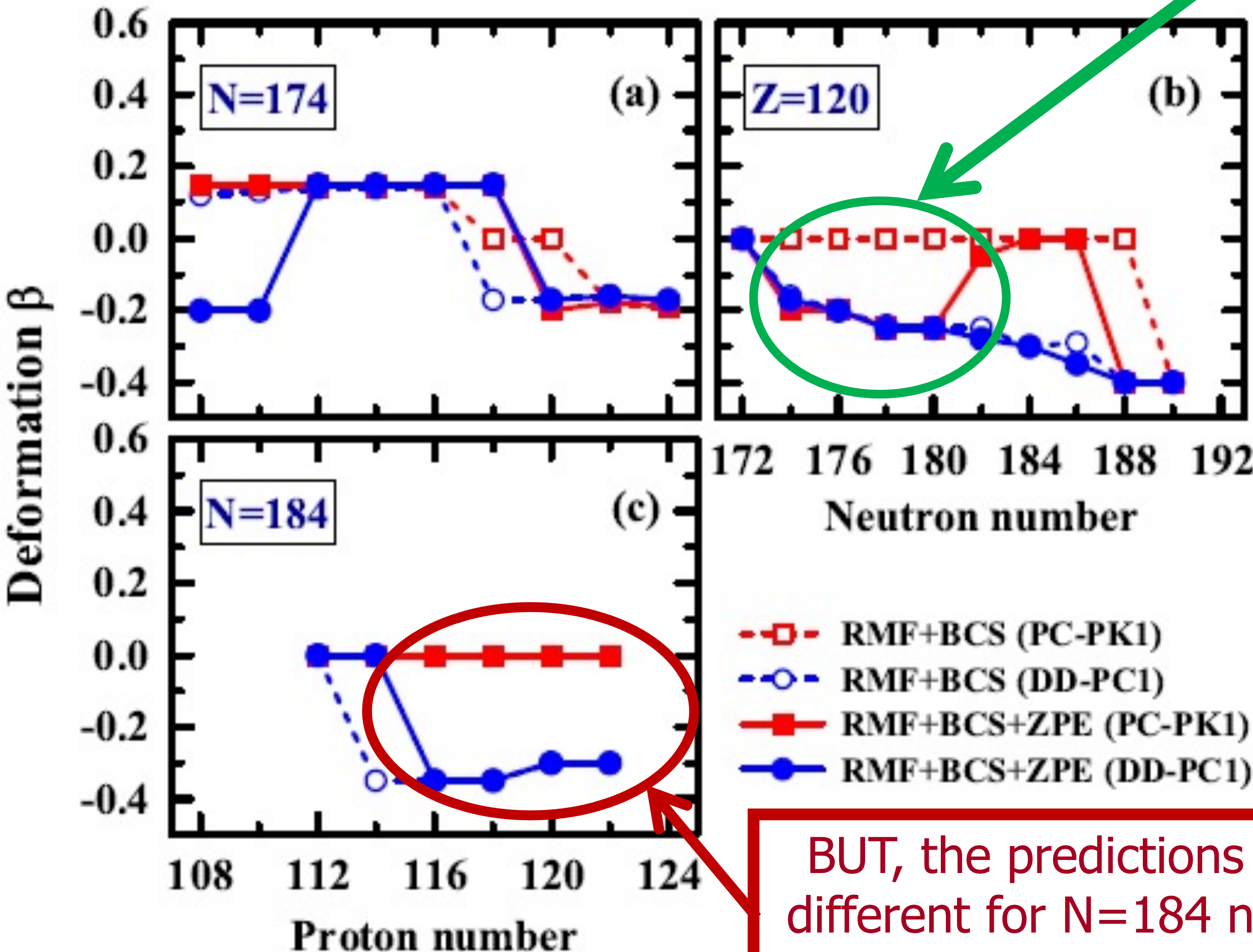

The inclusion of dynamical correlations brings the predictions ff DD-PC1 and PCPK1 functionals closer for nuclei along the Z=120 line

Z.Shi, AA, Z.P.Li J.Meng, PRC **99**, 064316 (2019)

BUT, the predictions remain distinctly different for N=184 nuclei even when dynamical correlations are included

Impact of the correlations beyond mean field on the ground states of SHE

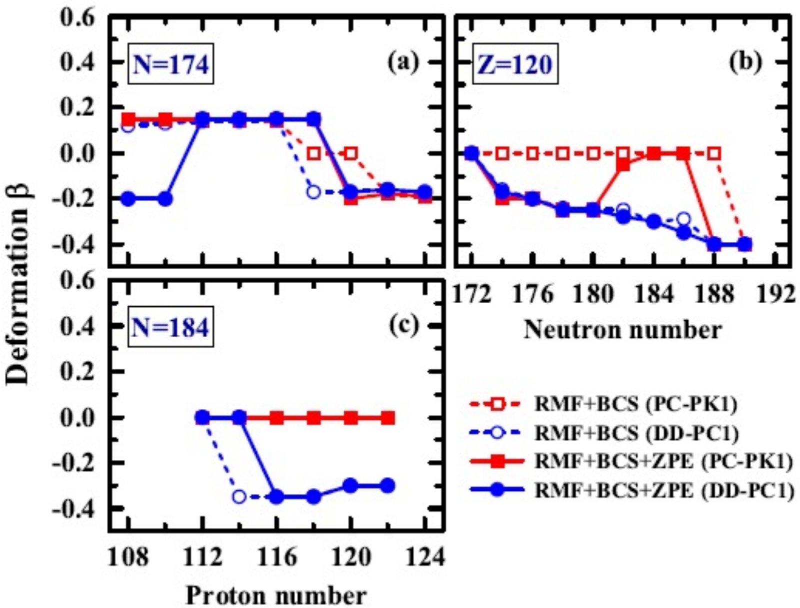

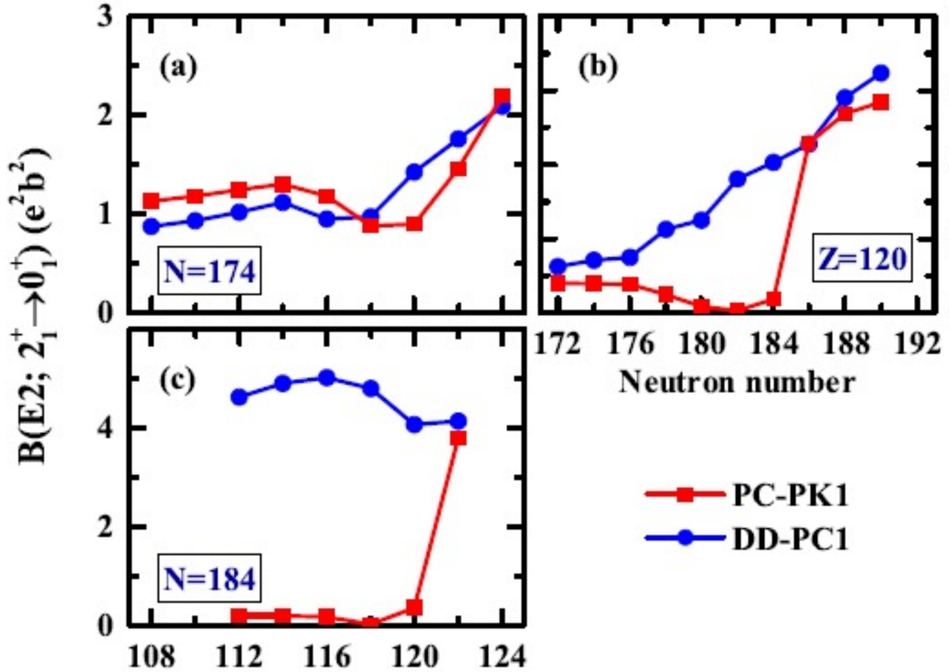

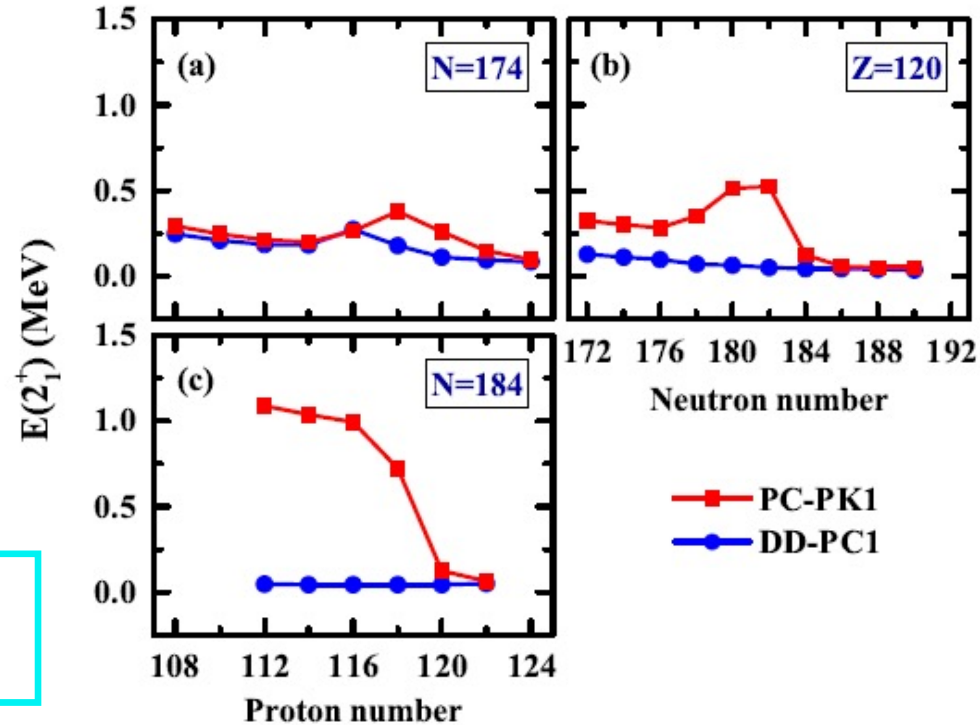

5 dimensional collective Hamiltonian (5DCH)

Z.Shi, AA, Z.P.Li J.Meng, PRC **99**, 064316 (2019)

The consequences for 96Zr

How reliable and unique is the interpretation of ground state in ^{96}Zr

Yu-Ting Rong, Bing-Nan Lu,
Static octupole deformations in ^{96}Zr from angular momentum and parity projections,
arXiv:2201.02114v1

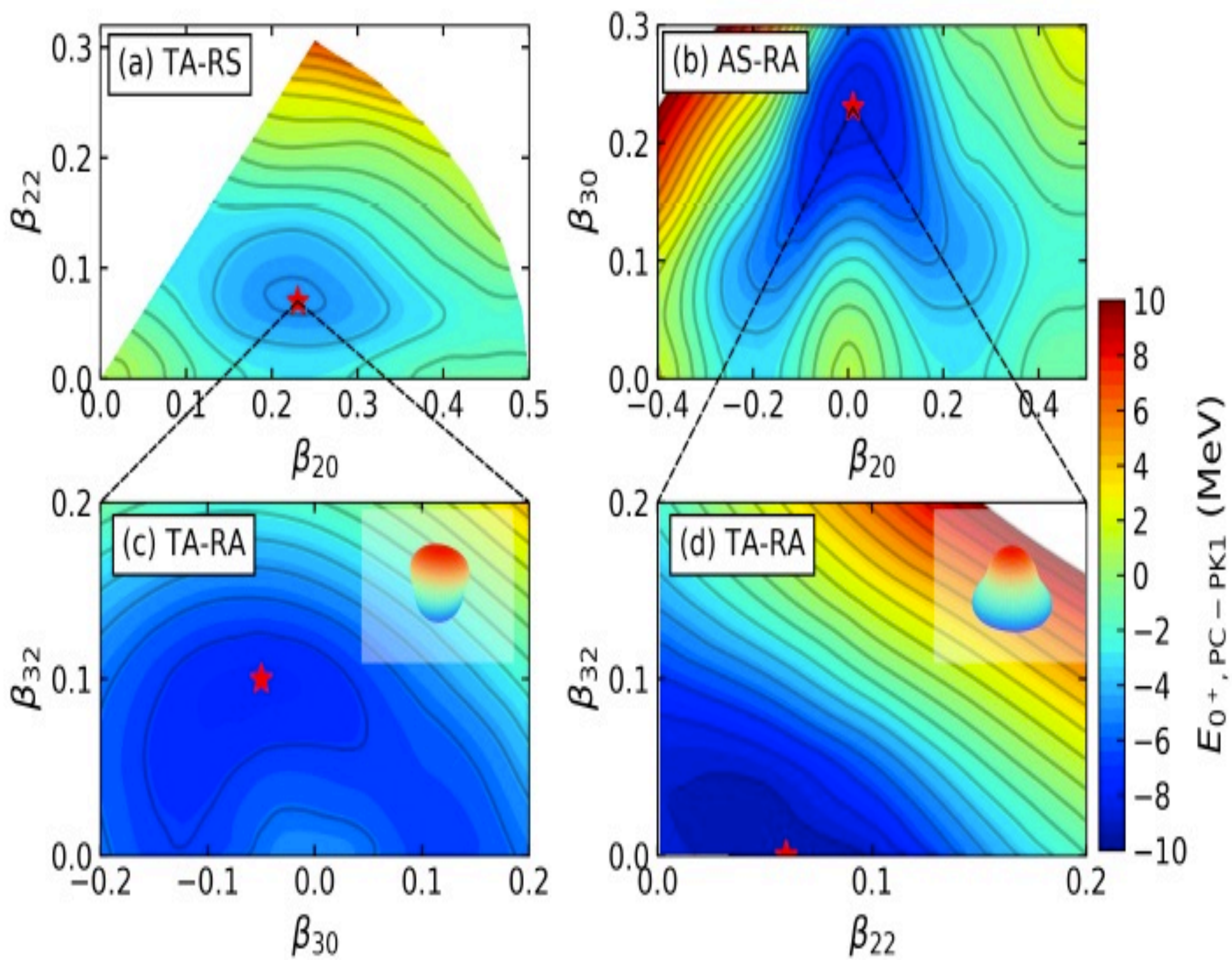

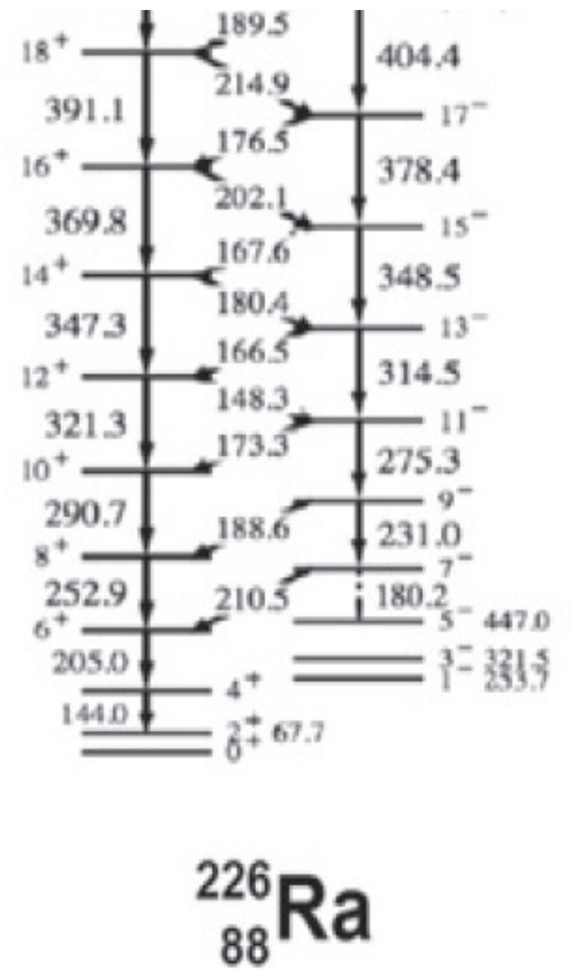

How reliable and unique is the interpretation of ground state in ^{96}Zr

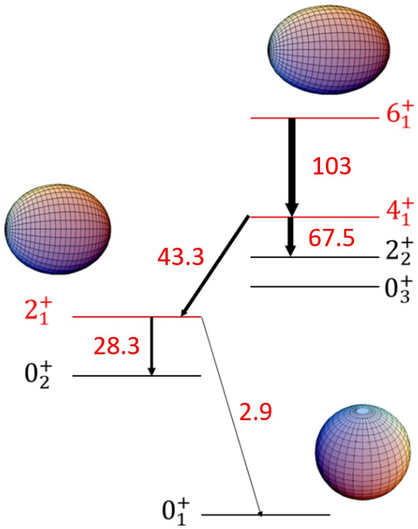

^{98}Zr: triple shape coexistence in ^{98}Zr.
ground state = spherical
PRL 121, 192501 (2018)

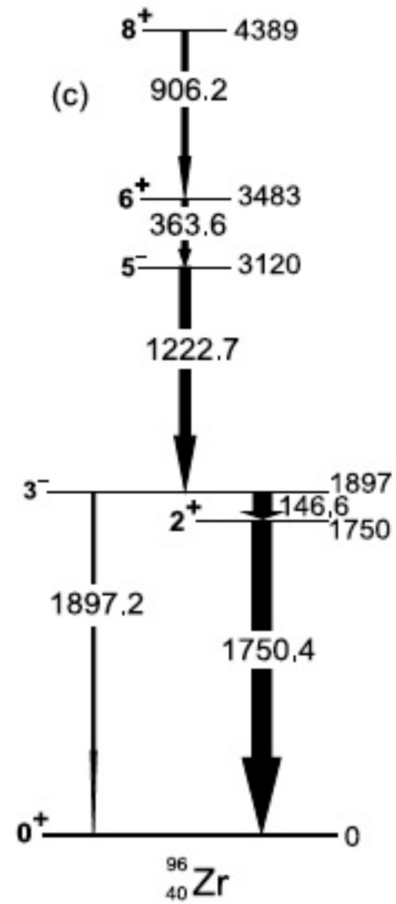

^{96}Zr: PLB 788, 396 (2019)
- reduced B(E3, $3^- \rightarrow 0^+$) strength
- Monte Carlo shell model calculations indicate that it is due to octupole vibrations

Conclusions

Theoretical results are subject to theoretical uncertainties especially in the cases of transition from one shape to another with change of proton and neutron numbers and in the case of octupole deformation.

Thus, model predictions have to be confronted with experimental data. However, the situation is complicated by the fact that no clear experimental measure of dynamical octupole deformation admixture to the ground state exist.

This material is based upon work supported by the U.S. Department of Energy, Office of Science, Office of Nuclear Physics under Award No. DE-SC0013037.